Atmos. Chem. Phys., 23, 2119–2143, 2023
https://doi.org/10.5194/acp-23-2119-2023

Atmospheric Chemistry and Physics
Open Access
EGU

Measurement report: Chemical components and ^{13}C and ^{15}N isotope ratios of fine aerosols over Tianjin, North China: year-round observations

Zhichao Dong, Chandra Mouli Pavuluri, Zhanjie Xu, Yu Wang, Peisen Li, Pingqing Fu, and Cong-Qiang Liu

Institute of Surface-Earth System Science, School of Earth System Science, Tianjin University, Tianjin 300072, China

Correspondence: Chandra Mouli Pavuluri (cmpavuluri@tju.edu.cn)

Received: 18 April 2022 – Discussion started: 22 June 2022
Revised: 29 November 2022 – Accepted: 13 January 2023 – Published: 13 February 2023

Abstract. To better understand the origins and seasonality of atmospheric aerosols in North China, we collected fine aerosols ($PM_{2.5}$) at an urban site (Nankai District, ND) and a suburban site (Haihe Education Park, HEP) in Tianjin from July 2018 to July 2019. The $PM_{2.5}$ was studied for carbonaceous, nitrogenous and ionic components and stable carbon and nitrogen isotope ratios of total carbon ($\delta^{13}C_{TC}$) and nitrogen ($\delta^{15}N_{TN}$). On average, the mass concentrations of $PM_{2.5}$, organic carbon (OC), elemental carbon (EC) and water-soluble OC (WSOC) were higher in winter than in summer at both ND and HEP. SO_4^{2-}, NO_3^- and NH_4^+ were the dominant ions, and their sum accounted for 89 % of the total ionic mass at ND and 87 % at HEP. NO_3^- and NH_4^+ peaked in winter and were at their minimum in summer, whereas SO_4^{2-} was higher in summer than in all the other seasons at HEP and was comparable among the seasons, although it peaked in winter at ND. $\delta^{13}C_{TC}$ and $\delta^{15}N_{TN}$ were −26.5 ‰ to −21.9 ‰ and +1.01 ‰ to +22.8 ‰ at ND and −25.5 ‰ to −22.8 ‰ and +4.91 ‰ to +18.6 ‰ at HEP. Based on seasonal variations in the measured parameters, we found that coal and biomass combustion emissions are the dominant sources of $PM_{2.5}$ in autumn and winter, while terrestrial and/or marine biological emissions are important in spring and summer in the Tianjin region, North China. In addition, our results implied that the secondary formation pathways of secondary organic aerosols in autumn/winter were different from those in spring/summer; i.e., they might be driven by NO_3 radicals in the former period.

1 Introduction

Atmospheric aerosols are mainly composed of carbonaceous and inorganic components such as elemental carbon (EC), organic matter (OM), sulfate (SO_4^{2-}), nitrate (NO_3^-), ammonium (NH_4^+), sea salt and minerals, each usually accounting for about 10 %–30 % of the aerosol mass load that generally ranges from 1 to 100 $\mu g\,m^{-3}$ (Pöschl, 2006; Pavuluri et al., 2015b). They have severe impacts on the Earth's climate system, air quality, visibility (Laden et al., 2000; Samet et al., 2000; Chow et al., 2002) and human health (Wessels et al., 2010). Aerosols can affect the climate directly by absorbing and scattering solar radiation and indirectly by acting as cloud condensation nuclei (CNN), and thus the hydrological cycle, at local, regional and global scales (Menon et al., 2002; Chow et al., 2006; Ramanathan et al., 2001). It has been recognized that ambient aerosol pollution is one of the major reasons for cancer (Y. Wang et al., 2016a) and other diseases in humans. According to the global burden of disease (GBD) 2010 comparative risk assessment, it has been estimated that fine aerosol ($PM_{2.5}$) pollution is causing a death rate of about 3 million people worldwide per year (Lim et al., 2012), and the total number of deaths per day is increasing by ∼ 1.5 % for every 10 $\mu g\,m^{-3}$ increase in the average $PM_{2.5}$ loading over 2 d (Schwartz et al., 1996). Therefore, it is important to explore the source and formation processes of the $PM_{2.5}$.

Carbonaceous components, EC and organic carbon and matter (OC and OM), account for about 20 %–50 % of $PM_{2.5}$ mass (Cui et al., 2015; Sillanpää et al., 2005). EC is directly emitted from incomplete combustion of fossil fuels and biomass burning (Robinson et al., 2007; Larson and Cass, 1989), while organic aerosols (OA, generally measured as OC) can be directly emitted into the atmosphere from combustion sources, soil dust and biota (primary OC, POC) and can also be produced from volatile organic compounds (VOCs) by photochemical reactions in the atmosphere to form secondary OC (SOC) (Robinson et al., 2007). It has been estimated that OC and EC emissions have been increased by 29 % and 37 %, i.e., from 2127 and 1356 Gg in 2000 to 2749 and 1857 Gg in 2012, respectively, in China (Jimenez et al., 2009; Cui et al., 2015). Previous studies have reported very high loadings of OC and EC in large cities in China, particularly the Beijing–Tianjin–Hebei (Yang et al., 2011; Duan et al., 2005; Zhao et al., 2013; Dan et al., 2004), Yangtze River Delta (Huang et al., 2013; Feng et al., 2006, 2009; Wang et al., 2010) and Pearl River Delta (Huang et al., 2012) regions, which are densely populated and economically developed. EC has a graphite-like structure and has been recognized as a major carbonaceous component of light absorption (Zhao et al., 2013), while OC is generally considered to be a major contributor to light scattering and cooling of the atmosphere and affects cloud properties, with direct and indirect effects on the radiative forcing (Yang et al., 2011). In addition, OC contains a variety of organic compounds, such as polycyclic aromatic hydrocarbons and other harmful components that cause severe human health risks (J. Wang et al., 2016). Moreover, studies have found that the loading of SOC is significant in $PM_{2.5}$ that has been influenced by long-range atmospheric transportation of the air masses (Bikkina et al., 2017b). Many recent laboratory and field observations highlighted the importance of liquid-phase photochemical oxidation reactions in forming secondary organic aerosol (SOA) in atmospheric waters (McNeill et al., 2012; Perri et al., 2010), and hence the loading of water-soluble OC (WSOC) is increased with photochemical aging of the aerosols, which further enhances the indirect effects of the SOA.

Since industrialization, the annual production of reactive nitrogen (N_r) has more than doubled due to combustion of fossil fuels and production of nitrogen fertilizers and other industrial products (Gu et al., 2013). Global N_r has dramatically increased from 15 Tg N yr^{-1} in 1860 to 156 Tg N yr^{-1} in 1995 and then to 192 Tg N yr^{-1} in 2008, significantly exceeding the annual natural production from terrestrial ecosystems (40–100 Tg N yr^{-1}) (Gu et al., 2013). The consumption of Haber–Bosch N fixatives (HBNFs) is high (35 Tg) for agricultural and industrial applications in China, which account for about 30 % of the world's total HBNF consumption (Gu et al., 2015; Galloway et al., 2008). The N_r species such as nitrogen oxides (NO_x: NO_2 and NO) and ammonia (NH_3) participate in a series of physical and chemical transformations, and 60 %–80 % of them convert to nitrogen-containing aerosols, affecting a variety of chemical reactions in the atmosphere (Fajardie et al., 1998). The photochemical cycle of NO_x provides an important precursor for the formation of ozone. In addition, NO_x can oxidize the hydrocarbons to aldehydes, ketones, acids and peroxyacetyl nitrate (PAN), leading to the formation of photochemical smog that affects the environment and human health (Wolfe and Patz, 2002). On the other hand, NH_3 is an important alkaline gas in the atmosphere and affects the optical properties, pH and CCN activity of aerosols and thus can influence the energy balance of the Earth's atmosphere (Bencs et al., 2010). It has also been established that secondary inorganic ions (SNA: $SO_4^{2-} + NO_3^- + NH_4^+$) are the main water-soluble inorganic ionic substances, which can directly affect the acidity of atmospheric precipitation, causing serious impacts on the ecological environment (Andreae et al., 2008) in addition to the impacts on the Earth's climate system.

Organic nitrogen (ON) is another form of N in atmospheric aerosols, such as semi-volatile amines, proteins and organic macromolecules. Water-soluble organic nitrogen (WSON), as an atmospheric input of the bioavailable nitrogen to the ecosystems, has also attracted attention in recent times (Matsumoto et al., 2018). In fact, aerosol ON is produced in the atmosphere by several secondary processes of VOCs and gaseous N species emitted from different sources (Ottley and Harrison, 1992; Utsunomiya and Wakamatsu, 1996). In addition to emissions from natural sources (such as soil and the ocean), ON can be generated by the reactions of secondary inorganic substances (SO_4^{2-}, NO_3^-, NH_4^+) with existing primary organic aerosol (POA) and SOA in the atmosphere. Therefore, it is difficult to understand the origins of aerosols C and N from only the measurement of their species and/or specific markers.

It is well known that the stable C ($\delta^{13}C_{TC}$) and N ($\delta^{15}N_{TN}$) isotope ratios of total C (TC) and nitrogen (TN) depend on their sources, with an obvious difference in the isotopic composition of the particles derived from different sources in the given specific area (Freyer, 1978; Moore, 1974). The particles of marine origin are highly enriched with ^{13}C and ^{15}N (Chesselet et al., 1981; Cachier et al., 1986; Miyazaki et al., 2011), which are distinct from those of the particles of continental origin, particularly anthropogenic sources such as coal combustion and vehicular emissions and the burning of C_3 plants as well (Cachier et al., 1986; Turekian et al., 1998; Martinelli et al., 2002; Widory, 2007; Cao et al., 2011). However, the ^{13}C is enriched in the particles emitted from C_4 plant burning, while the ^{15}N is enriched in those of terrestrial biogenic origin, including the biomass burning of both C_3 and C_4 plants. It has been reported that the $\delta^{13}C_{TC}$ of −26.0 ‰ and −21.0 ‰ in atmospheric aerosols represents marine and continental origins, respectively (Turekian et al., 2003; Cachier et al., 1986), while $\delta^{15}N_{TN}$ in marine aerosols ranged from −2.2 ‰ to 8.9 ‰ (Miyazaki et al., 2011), the particles emitted from biomass burning of different C_3 and

C_4 plants ranged from 2.0‰ to 22.7‰ and those emitted from the combustion of fossil fuels such as unleaded gasoline, diesel and coal ranged from −19.4‰ to +5.4‰ (Martinelli et al., 2002; Pavuluri et al., 2010; Widory, 2007).

On the other hand, the unidirectional chemical reactions cause an enrichment of ^{12}C in reaction products resulting in the remaining reactants being isotopically heavier and the phase partitioning (gas to particle or vice versa, e.g., $NH_4^+ \leftrightarrow NH_3$) of a compound also resulting in isotopic fractionation (Hoefs, 1997). Furthermore, the chemical processing of aerosols results in the enrichment of ^{13}C (and ^{15}N) in the reaction product retained in the particle phase if some of the products are volatile (Turekian et al., 2003). Therefore, the $\delta^{13}C_{TC}$ and $\delta^{15}N_{TN}$ are modified by several chemical and physical processes in the atmosphere such as secondary aerosol formation and/or transformation (Kundu et al., 2010; Mkoma et al., 2014; Morin et al., 2009). However, such isotopic fractionation is more significant in the case of molecular species but insignificant in the case of TC and TN, because the TC and TN contents contain both the reactants and the products in the particle phase. In fact, the gas-to-particle and/or particle-to-gas transitions, even in the case of $NH_4^+ \leftrightarrow NH_3$, are not intensive, except under extreme temperatures (Pavuluri et al., 2010, 2011). Therefore, the $\delta^{13}C_{TC}$ and $\delta^{15}N_{TN}$ of $PM_{2.5}$ would provide insights, preferably into their origins. They can also provide insights into secondary formation and/or transformations of aerosols if the removal processes including physical transformation (particle to gas phase) are significant, which could result in the enrichment of ^{13}C and ^{15}N in the particles. Hence, the $\delta^{13}C_{TC}$ and $\delta^{15}N_{TN}$ of $PM_{2.5}$ are useful for better constraining the relative significance of such factors (Bikkina et al., 2017a; Pavuluri et al., 2010; Jickells et al., 2003; Martinelli et al., 2002). The application of $\delta^{13}C$ and $\delta^{15}N$ as potential tracers to investigate the origin and atmospheric processing (aging) of C and N species is well documented and has been applied in several studies in the last 2 decades (Kundu et al., 2010; Martinelli et al., 2002; Pavuluri et al., 2015c; Rudolph, 2002). However, it should be noted that the influence of isotopic fractionation by the aging on $\delta^{13}C_{TC}$ and $\delta^{15}N_{TN}$ values of $PM_{2.5}$ becomes insignificant when the local fresh air masses are mixed with the aged air masses that are transported from distant source regions and/or the aerosol removal processes are insignificant, despite the fact that the isotopic fraction must be significant at a molecular level.

Because of rapid economic growth, the aerosol loading is commonly observed to be high in China, particularly in the Beijing–Tianjin–Hebei region. According to the data analysis of the "2 + 26" list of urban industrial sources in 2018, primary emissions of $PM_{2.5}$, SO_2, NO_x and VOCs from industrial sources account for 60 %, 46 %, 23 % and 49 % of the total regional emissions, respectively. Moreover, the total land area of Tianjin is 11 966.45 km^2, with the agricultural land area 6894.41 km^2, accounting for 57.6 % of the total land area. According to the results of the 9th China forest resources inventory, Tianjin has 2039 km^2 of forest area (17.0 % of the total land area). In addition, there are 17 natural protected areas of various types, with a total area of about 1418.79 km^2 in Tianjin (https://www.tjrd.gov.cn/tjfq/system/2019/04/24/030012397.shtml, last access: 24 April 2019). Thus, Tianjin is surrounded by areas largely covered with agricultural fields and forests that emit large amounts of VOCs and bioaerosols. On the other hand, the East Asian monsoon climate prevailing over the region brings the long-range transported air masses to Tianjin, and their origins vary with the season (Wang et al., 2018). Therefore, the investigation of the Tianjin aerosols sources and formation processes provides better insights into the types of aerosol sources at a regional level, in addition to the local industrial and domestic pollutant emissions in North China. However, the studies on Tianjin aerosols are limited and mostly focused on the short-term measurements of mass concentrations of $PM_{2.5}$, EC, OC and/or inorganic ions (Kong et al., 2010; Li et al., 2009, 2012; X. Li et al., 2017) but not the long-term measurements and seasonal characterization of carbonaceous and nitrogenous components and water-soluble inorganic ions that are important for better understanding the sources and characteristics of the $PM_{2.5}$ (Cao et al., 2007; Dentener et al., 2006; Pavuluri et al., 2015b). Furthermore, ON, which represents a significant fraction (up to 80 %) of total aerosol N and plays an important role in biogeochemical cycles (Pavuluri et al., 2015a; Cape et al., 2011), has not been studied in Tianjin aerosols.

Therefore, the comprehensive study of various chemical components and $\delta^{13}C_{TC}$ and $\delta^{15}N_{TN}$ of $PM_{2.5}$ in Tianjin is highly needed in order to better understand their origins and even aging to some extent over the region. Here, we present the characteristics and seasonality of carbonaceous (EC, OC, WSOC, WIOC and SOC) and nitrogenous (IN, ON and WSON) components, inorganic ions (Cl^-, SO_4^{2-}, NO_3^-, Na^+, NH_4^+, K^+, Mg^{2+} and Ca^{2+}) and $\delta^{13}C_{TC}$ and $\delta^{15}N_{TN}$ in $PM_{2.5}$ collected over a 1-year period at an urban site and a suburban site in Tianjin, North China. Based on the chemical compositions, $\delta^{15}N_{TN}$ and $\delta^{13}C_{TC}$ and their seasonal changes, we discuss the origins and possible aging of $PM_{2.5}$ over the Tianjin region.

2 Materials and methods

2.1 Aerosol sampling and mass measurement

$PM_{2.5}$ sampling was performed at an urban site, Nankai District (ND), located in the central part at 39.11° N, 117.18° E, and a suburban (background) site, Haihe Education Park (HEP), located at 39.00° N, 117.32° E, 23 km away from ND, in Tianjin, a coastal metropolis located on the lower reaches of the Haihe River and the Bohai Sea in the Beijing–Tianjin–Hebei urban economic area in the northern part of the Chinese mainland (Fig. 1), with a population of ∼ 16 million (https://wiki.hk.wjbk.site, last access:

24 April 2019). The $PM_{2.5}$ sampling was conducted on the rooftop of a seven-storey teaching building of Tianjin University Weijin Road campus in ND for about 72 h (3 consecutive days), each sampled continuously from 5 July 2018 to 4 July 2019 using precombusted (450 °C, 6 h) quartz membrane (Pallflex 2500QAT-UP) filters and a high-volume air sampler (Tisch Environmental, TE-6070DX) with a flow rate of 1.0 m^3 min^{-1} ($n = 121$). Simultaneously, the $PM_{2.5}$ sampling was conducted on the rooftop of a six-storey teaching building of Tianjin University Peiyangyuan campus in HEP with the same sampling frequency (72 h each) for a 1-month period in each season: from 5 July–4 August in summer, 30 September–30 October in autumn 2018, 1 January–1 February in winter and 2 April–2 May in spring 2019. Prior to analysis, the filter samples were placed in a precombusted glass jar with a Teflon-lined cap and stored in the dark at −20 °C. A blank filter sample was also collected in each season following the same procedure without turning on the sampler pump and placing the filter in a filter hood for 10 min.

Each filter was dehumidified in a desiccator for 48 h before and after sampling, and the mass concentration of $PM_{2.5}$ was determined by gravimetric analysis.

It should be noted that $PM_{2.5}$ samples collected on quartz fiber filters might have positive sampling artifacts due to the adsorption of gas-phase organic and nitrogen compounds and the negative artifacts by evaporation of the semi-volatile organic and nitrogen species from the aerosol particles (Turpin et al., 2000; Schaap et al., 2004). Since the sampling time is long (∼ 72 h) in this study, the evaporation of semi-volatile species from the particles should be more effective than the adsorption of gaseous species by a quartz fiber filter, which would be saturated upon continuous sampling, and thus the reported concentrations may be underestimated. However, we consider that such losses should be minimal because the ambient temperatures encountered in Tianjin are rather low (see Sect. 3.1) and thus may not cause a significant evaporative loss (Schaap et al., 2004) during the sampling period. Therefore, we believe that our sampling technique does not have serious sampling artifacts even in summer, although we do not rule them out completely.

2.2 Chemical analyses

2.2.1 Measurements of carbonaceous components

OC and EC were measured using an OC/EC analyzer (USA, Sunset Laboratory Inc.) based on thermal light transmission following the IMPROVE protocol of the protective visual environment (Wan et al., 2017, 2015; Chow et al., 2007) and assuming the carbonate carbon was negligible (Pavuluri et al., 2011; Wang et al., 2019), because the C removed by HCl treatment has been reported to be only 6.3 % in TC at Gosan Island, South Korea (Kawamura et al., 2004), where the long-range transported air masses enriched with soil dust are the major sources, rather than anthropogenic sources, unlike in the Tianjin region. Briefly, an aliquot of a filter (1.5 cm^2) of each sample was punched and placed in a quartz boat in the thermal desorption chamber of the analyzer, and then the carbon content of each sample was measured by a two-step heating procedure. The analytical principle of the instrument has been described in detail in the literature (Cao et al., 2007; Watson et al., 2005). During the experiment, a sucrose solution with a known carbon content (3.6 μg C $μL^{-1}$) was used as a standard reference for the measurement of OC and EC. The analytical errors in duplicate analyses were within 2 % for OC and 5 % for EC.

The total organic carbon (TOC) analyzer (model: OI, 1030W + 1088) was used to measure the content of WSOC. Total inorganic carbon (TIC) obtained by acidizing the sample with HCl down to a pH of less than 2.0 and TOC obtained by wet oxidation, i.e., oxidizing the sample with an agent (e.g., persulfate) at 100 °C, can be measured simultaneously with the same sample, ensuring the highest detection accuracy and reliability of the data. An aliquot of a filter sample (one disc of 14 mm in diameter for filters 1–65 and 22 mm for filters 66–172) was extracted into 20 and 30 mL organic-free Milli-Q water, respectively, under ultrasonication for 20 min (Wang et al., 2019). The extracts were filtered through a 0.22 μm polytetrafluoroethylene (PTFE) syringe filter, and then the content of the WSOC was measured using the TOC analyzer. The analytical uncertainty in measurements was generally less than 5 %. The concentrations of OC, EC and WSOC were corrected for field blanks.

The sum of OC and EC was considered to be TC, and the difference between OC and WSOC was considered to be the water-insoluble OC (WIOC) (Wang et al., 2018).

Due to a lack of analytical methods to directly measure SOC (Turpin and Huntzicker, 1995), the SOC was estimated using the OC/EC tracer-based method proposed by Turpin et al. (2000). The formula for its calculation is as follows:

$$SOC = OC - (EC \times (OC/EC)_{pri}),$$

where $(OC/EC)_{pri}$ is the mass concentration ratio between OC and EC generated by primary emission, which is generally the minimum value among the measured OC/EC. Because the OC/EC is highly influenced by meteorological conditions, emission sources and other factors and thus the estimation of SOC using the minimum value results in a large deviation, we used the average value of three minimum values in the OC/EC ratios as the $(OC/EC)_{pri}$, which was 6.71 at ND and 4.62 at HEP.

2.2.2 Measurements of inorganic ions

Inorganic ions Cl^-, SO_4^{2-}, NO_3^-, Na^+, NH_4^+, K^+, Mg^{2+} and Ca^{2+} were measured using ion chromatography (ICS-5000 System, China, Dai An). An aliquot of a filter sample (one disc of 22 mm in diameter) was extracted into 30 mL Milli-Q water under ultrasonication for 30 min and filtered

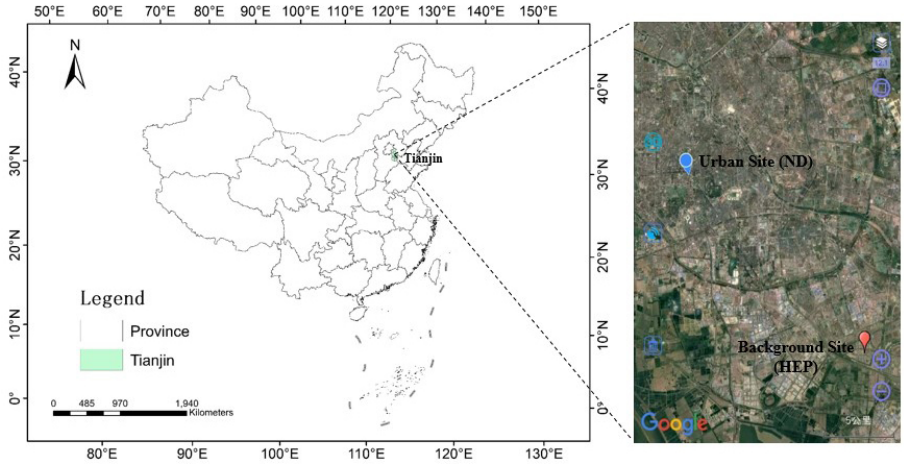

Figure 1. Map of China with the study area, Tianjin, North China. The sampling points located in urban (ND) and suburban (HEP) locations are shown in the inset. (The map in the inset was generated using © Google Maps.)

with a PTFE syringe filter (0.22 µm) and then injected into an ion chromatograph. A mixture of $NaHCO_3$, Na_2CO_3, NaOH (50 % NaOH solution) eluent and an IonPac AG11-HC/AS11-HC column and a 30 mM KOH suppresser with a flow rate of 1.2 mL min^{-1} was used for anion measurement. For cationic measurement, methyl sulfonic acid and IonPac CS12A and CG12A columns at a flow rate of 1.0 mL min^{-1} with a 20 mM mesylate suppressor were used. The analytical error in duplicate analyses was generally less than 5 %. Concentrations of all the ions were corrected for field blanks.

2.2.3 Determination of nitrogenous components

Water-soluble total nitrogen (WSTN) was determined using a continuous-flow analyzer (CFA, Skalar, the Netherlands, San++) following the standard procedure. Briefly, an aliquot of a filter (3.80 cm^2) sample was extracted into 10 mL Milli-Q water under ultrasonication for 10 min each three times, and the extracts were filtered through 0.22 µm-sized Teflon syringe filters to remove filter debris. The filter extracts were then mixed with excess potassium persulfate and digested in the UV digester to convert all N to NO_3^- and passed through a reduction column equipped with a granular copper and cadmium column to reduce NO_3^- to nitrite (NO_2^-). The produced nitrite is reacted with aminobenzene sulfonic acid to result in high molecular weight nitrogen compounds (azo dye), and then the absorbance of total N was measured at 540 nm. The average analysis error of the repeated analysis was 167.1 %. Such a large analytical error can be attributed to the slightly low reproducibility of the instrument with the detection limit of 0.01–5 mg L^{-1} and the uneven distribution of particles in the sampling filter.

The N contents of NO_2^-, NO_3^- and NH_4^+ were calculated from their concentrations by multiplying them by the percent factor of N in the given molecule. The sum of those contents was considered to be the total inorganic nitrogen (IN). The difference between the concentrations of WSTN and IN was considered to be WSON (Matsumoto et al., 2018):

$$\mathrm{WSON} = \mathrm{WSTN} - \mathrm{IN}.$$

However, it should be noted that the analytical uncertainties associated with the measurements of WSTN and NO_2^-, NO_3^- and NH_4^+ must result in huge error in the estimation of WSON. The propagating error in WSON estimation from duplicate analysis of the samples for NO_3^-, NH_4^+ and WSTN with uncertainties of 0.78 %, 1.82 % and 16.1 %, respectively, was 0.83. However, we consider that such errors may not influence the conclusions drawn from this study, because they were drawn based on the temporal trends rather than the absolute concentrations.

2.2.4 Determination of stable carbon and nitrogen isotope ratios of TC ($\delta^{13}C_{TC}$) and TN ($\delta^{15}N_{TN}$)

$\delta^{13}C_{TC}$ and $\delta^{15}N_{TN}$ were determined using an elemental analyzer (EA, Flash 2000HT) coupled with a stable isotope ratio mass spectrometer (IRMS, 253 Plus). Briefly, an aliquot of a filter was subjected to acid steaming and placed in a dry dish containing concentrated HNO_3 for 12 h to remove inorganic carbon ($CaCO_3$) content, if any, which affects the result of the $\delta^{13}C_{TC}$. The acidified filter sample was dried out in an oven for 24 h and then packed into a tin cup that was injected into EA. The derived gases CO_2 and N_2 were transferred into IRMS through ConFlo-II to measure the $^{13}C/^{12}C$ in TC and $^{15}N/^{14}N$ in TN.

The isotope ratios of $^{13}C/^{12}C$ and $^{15}N/^{14}N$ are expressed as delta (δ) values ($\delta^{13}C_{TC}$ and $\delta^{15}N_{TN}$) after the normalization with Pee Dee Belemnite (PDB) and atmospheric N_2 in parts per million (Duarte et al., 2019; Li et al., 2022). The $\delta^{13}C_{TC}$ and $\delta^{15}N_{TN}$ were calculated using the following for-

mulas (Fu et al., 2012; Pavuluri et al., 2010):

$$\delta^{13}C_{TC} = [(^{13}C/^{12}C)_{sample}/(^{13}C/^{12}C)_{standard} - 1] \times 1000,$$
$$\delta^{15}N_{TN} = [(^{15}N/^{14}N)_{sample}/(^{15}N/^{14}N)_{standard} - 1] \times 1000.$$

2.3 Measurements of meteorological parameters, simulations of air mass trajectories, and data statistical analyses

The meteorology data from Tianjin were collected from a mobile weather station (Gill MetPak, UK) installed at the sampling site during the campaign in this study. Five-day backward air mass trajectory clustering analysis was conducted using the NOAA HYLSPLIT modeling system (https://www.ready.noaa.gov/HYSPLIT.php, last access: 15 June 2020) for every month to identify the source regions of the air parcels that arrived over Tianjin at 500 m a.g.l. (above the ground level) at a regional scale during the campaign. The statistical analysis of the obtained data was performed using Igor Pro 7 (WaveMatrics Inc., OR, USA) software. A summary of the statistics and linear analysis has been carried out in order to characterize the variations in individual measurements as well as to estimate the relation between the considered parameters.

3 Results and discussion

3.1 Meteorology and backward air mass trajectories

Temporal variations in the averages of the data for each sample period are depicted in Fig. 2. The ambient temperature, relative humidity (RH) and wind speed showed a clear seasonal pattern (Fig. 2). On average, the temperature was higher (27.3 °C) in summer and lower (1.28 °C) in winter. The annual average of RH was 39.2 %. It was relatively higher in summer and autumn than that in winter and spring. The average wind speed in autumn (2.03 m s^{-1}) was almost similar to that in spring (2.06 m s^{-1}) but was lower in summer (1.64 m s^{-1}) and winter (1.58 m s^{-1}).

Plots of 5 d backward air mass trajectory clusters are depicted in Fig. 3. The trajectories showed that most of the air masses that arrived in Tianjin originated from the oceanic region in summer (Fig. 3). In particular, 50 % of the air masses originated from the East Sea in July 2018, while a small portion (8 %) of the air masses originated from Northeast China and Siberia, whereas in autumn, winter and spring, they mostly originated from Siberia and Mongolia as well as from inland China (Fig. 3). It is noteworthy that 33 % of the air masses arrived in Tianjin during September, and 28 % during October originated from the northern parts of China. Therefore, the chemical composition and characteristics of $PM_{2.5}$ in Tianjin should have been significantly influenced by the long-range transported air masses and varied according to seasonal changes in addition to the local emissions.

3.2 Concentrations and seasonal variations of $PM_{2.5}$

Concentrations of $PM_{2.5}$ and its carbonaceous components EC, OC, SOC, WSOC, WIOC and TC, nitrogenous components WSTN, IN and WSON, inorganic ions (Cl^-, NO_3^-, SO_4^{2-}, Na^+, K^+, NH_4^+, Ca^{2+} and Mg^{2+}) as well as $\delta^{13}C_{TC}$ and $\delta^{15}C_{TN}$ during the whole campaign (annual) and in each season at ND and HEP in Tianjin, North China, are summarized in Table 1. Generally, $PM_{2.5}$ levels are controlled by emissions, transport and chemical transformation and deposition processes, all of which are influenced by meteorological conditions (Yang et al., 2011; Zhang et al., 2013). The temporal trend of $PM_{2.5}$ was found to be similar to that of RH and opposite to that of wind speed (Figs. 2 and 4). On average, the concentrations of $PM_{2.5}$ at ND and HEP in winter were 4 and 3 times higher than that in summer (Table 1). According to the China ambient air quality standard (GB3095-2012), the average $PM_{2.5}$ concentration limit in the ambient environment is 75 µg m^{-3} for 24 h and 35 µg m^{-3} for the year. Although the annual average concentration of $PM_{2.5}$ in Tianjin did not exceed the national $PM_{2.5}$ limit, it is about 3 times higher than that of the global limit (10 µg m^{-3}) stipulated by the World Health Organization. Furthermore, the average concentration of $PM_{2.5}$ was found to be higher in spring than in autumn (Table 1), probably due to enhanced eruption of dust from open lands by relatively strong winds in spring (Fig. 2). In addition, the long-range transported air masses that passed over the Mongolian region must have been enriched with the soil dust, resulting in the higher levels of $PM_{2.5}$ in spring in Tianjin. In fact, the dust storms over Mongolia and China that are common in spring enhance the loading of $PM_{2.5}$ in the East Asian atmosphere (Liu et al., 2011).

However, the average $PM_{2.5}$ concentration found in this study is significantly lower than that (109.8 µg m^{-3}) reported 10 years before in Tianjin (Li et al., 2009). Furthermore, it is also lower than that reported in Harbin, Northeast China, but similar to that recorded in the southeastern coastal cities in China: Ningbo and Guangzhou (Table 2). Such a relatively lower concentration of $PM_{2.5}$ in Tianjin is likely, because the government is strictly implementing various control measures, including the replacement of coal with natural gas and electricity (http://huanbao.bjx.com.cn/news/20170901/847140.shtml, last access: 1 September 2017) in air pollutant emissions in North China since 2013. It has been reported that the average concentration of $PM_{2.5}$ decreased from 2011 to 2017 in the southwestern city of Chengdu, consistent with the variation trend of $PM_{2.5}$ concentrations in most cities in North China (Table 2), which indicates that the government's measures for prevention and control of air pollution are effective in China. However, the $PM_{2.5}$ loading over most Chinese cities, including Tianjin, is still much higher compared to that reported in the USA (Table 2). Such comparisons indicate that the aerosol loading is significantly high in the Tianjin atmosphere and needs to continue the en-

Table 1. Summary of concentrations of carbonaceous (EC, OC, SOC, WSOC, WIOC and TC), nitrogenous (WSTN, IN and WSON) and inorganic ionic (Cl^-, NO_3^-, SO_4^{2-}, Na^+, K^+, NH_4^+, Ca^{2+} and Mg^{2+}) components ($\mu g\,m^{-3}$) and stable carbon and nitrogen isotope ratios (‰) of total carbon ($\delta^{13}C_{TC}$) and nitrogen ($\delta^{15}C_{TN}$) in fine aerosols together with the $PM_{2.5}$ mass ($\mu g\,m^{-3}$) at urban (ND) and suburban (HEP) sites in Tianjin, North China, on 5 July 2018 and 5 July 2019.

Components	Annual		Summer		Autumn		Winter		Spring	
	Range/med	Avg ± SD	Range/med	Avg ± SD	Range/med	Avg ± SD	Range/med	Avg ± SD	Range/med	Avg ± SD
	ND ($n = 121$) HEP ($n = 40$)		ND ($n = 30$, Jun–Aug) HEP ($n = 10$, Jul)		ND ($n = 30$, Sep–Nov) HEP ($n = 10$, Oct)		ND ($n = 30$, Dec–Feb) HEP ($n = 10$, Jan)		ND ($n = 31$, Mar–May) HEP ($n = 10$, Apr)	
Carbonaceous components ($\mu g\,m^{-3}$)										
EC	0.10 to 0.56/0.26 0.09 to 0.81/0.40	0.27 ± 0.11 0.40 ± 0.18	0.11 to 0.31/0.18 0.09 to 0.59/0.27	0.18 ± 0.05 0.28 ± 0.16	0.21 to 0.54/0.33 0.41 to 0.81/0.61	0.36 ± 0.10 0.59 ± 0.13	0.10 to 0.56/0.28 0.15 to 0.53/0.39	0.30 ± 0.10 0.37 ± 0.10	0.10 to 0.34/0.25 0.18 to −0.62/0.32	0.24 ± 0.07 0.36 ± 0.15
OC	1.37 to 24.7/3.40 0.85 to 14.7/4.40	4.93 ± 3.79 5.61 ± 3.55	1.37 to 3.26/2.31 0.85 to 4.34/2.25	2.31 ± 0.52 2.44 ± 1.20	1.48 to 12.8/4.44 3.01 to 9.86/4.62	5.00 ± 2.65 5.28 ± 2.07	2.49 to 24.7/7.97 7.18 to 14.7/9.51	8.79 ± 4.85 10.4 ± 2.98	1.52 to 6.58/3.38 2.46 to 5.68/4.39	3.36 ± 1.12 4.30 ± 1.11
WSOC	0.69 to 16.0/2.56 0.66 to 9.44/3.52	3.25 ± 2.18 3.47 ± 2.04	1.14 to 3.12/1.74 0.66 to 3.73/1.81	1.88 ± 0.53 2.16 ± 1.17	1.16 to 7.68/3.13 1.48 to 6.11/2.93	3.45 ± 1.74 3.08 ± 1.41	1.37 to 16.0/4.19 4.00 to 9.44/5.50	5.06 ± 2.99 4.00 to 9.44	0.69 to 4.03/2.44 0.95 to 4.38/2.44	2.48 ± 0.82 2.70 ± 1.18
WIOC	0.00 to 8.93/1.01 0.00 to 7.39/1.77	1.68 ± 1.77 2.14 ± 1.75	0.00 to 1.33/0.38 0.00 to 0.67/0.22	0.43 ± 0.32 0.29 ± 0.21	0.21 to 5.07/1.37 0.61 to 3.75/2.26	1.55 ± 1.04 2.20 ± 0.86	0.00 to 8.93/3.33 3.02 to 7.39/3.93	3.74 ± 2.09 4.48 ± 1.45	0.23 to 2.62/0.73 0.51 to 3.15/1.43	0.88 ± 0.63 1.60 ± 0.70
SOC	0.00 to 20.9/1.65 0.00 to 12.8/2.86	3.11 ± 3.43 3.75 ± 3.48	0.24 to 1.75/1.13 0.00 to 2.97/0.71	1.08 ± 0.37 1.18 ± 1.01	0.00 to 10.7/2.24 0.05 to 6.73/2.56	2.59 ± 2.58 2.56 ± 2.15	1.58 to 20.9/5.92 5.46 to 12.8/8.48	6.78 ± 4.35 8.68 ± 2.90	0.83 to 4.88/1.51 1.04 to 4.18/2.67	1.73 ± 0.87 2.63 ± 1.08
WSOC/OC	0.30 to 1.05/0.72 0.30 to 1.04/0.61	0.71 ± 0.15 0.66 ± 0.17	0.54 to 1.05/0.80 0.77 to 1.04/0.84	0.82 ± 0.12 0.87 ± 0.09	0.43 to 0.92/0.70 0.47 to 0.85/0.57	0.70 ± 0.10 0.58 ± 0.11	0.41 to 1.05/0.57 0.46 to 0.67/0.58	0.57 ± 0.11 0.57 ± 0.07	0.30 to 0.93/0.79 0.30 to 0.82/0.62	0.75 ± 0.14 0.61 ± 0.17
OC/EC	6.56 to 48.1/14.4 4.01 to 63.0/12.4	17.8 ± 9.46 15.7 ± 11.5	7.64 to 16.2/13.3 4.01 to 14.9/10.1	13.1 ± 2.18 9.67 ± 3.62	6.56 to 41.7/12.5 4.67 to 14.5/10.3	14.5 ± 8.39 9.31 ± 3.70	16.1 to 48.1/28.1 16.1 to 63.0/29.5	29.2 ± 9.73 30.4 ± 13.1	9.37 to 25.9/13.3 6.28 to 19.7/13.2	14.1 ± 3.18 13.2 ± 4.70
SOC/OC	0.00 to 0.86/0.53 0.00 to 0.93/0.63	0.53 ± 0.20 0.57 ± 0.25	0.12 to 0.58/0.49 0.00 to 0.69/0.54	0.47 ± 0.11 0.46 ± 0.22	0.00 to 0.84/0.46 0.01 to 0.68/0.55	0.41 ± 0.26 0.41 ± 0.26	0.58 to 0.86/0.76 0.71 to 0.93/0.84	0.74 ± 0.08 0.82 ± 0.07	0.28 to 0.74/0.49 0.27 to 0.77/0.65	0.50 ± 0.09 0.60 ± 0.16
Nitrogenous components ($\mu g\,m^{-3}$)										
WSTN	0.32 to 26.3/3.15 1.34 to 18.4/6.25	5.45 ± 5.50 7.34 ± 5.13	0.56 to 4.57/1.73 1.37 to 6.61/3.93	1.77 ± 0.86 3.64 ± 1.57	0.32 to 24.9/5.47 1.57 to 18.2/5.92	6.63 ± 6.06 7.23 ± 5.90	1.52 to 26.3/5.84 4.68 to 18.4/7.94	8.51 ± 6.40 9.68 ± 4.20	0.73 to 16.1/3.33 1.34 to 17.5/8.57	4.80 ± 4.03 8.80 ± 5.67
IN	0.00 to 26.5/3.35 1.39 to 14.8/5.40	5.21 ± 5.01 6.14 ± 3.90	0.00 to 5.67/1.79 1.40 to 5.43/3.54	1.82 ± 0.96 3.32 ± 1.17	0.19 to 21.3/5.32 1.39 to 14.5/6.43	6.10 ± 5.38 6.45 ± 4.61	1.86 to 26.5/5.82 4.24 to 14.2/6.81	8.23 ± 5.91 7.98 ± 3.08	1.00 to 16.0/3.50 1.61 to 14.8/5.97	4.68 ± 3.55 6.82 ± 4.32
WSON	0.00 to 3.51/0.72 0.00 to 9.80/0.77	0.40 ± 0.69 1.29 ± 1.47	0.00 to 0.39/0.03 0.00 to 1.18/0.43	0.07 ± 0.09 0.47 ± 0.36	0.00 to 3.51/0.31 0.00 to 3.65/0.10	0.63 ± 0.83 1.01 ± 1.46	0.00 to 2.32/0.01 0.44 to 4.18/1.18	0.40 ± 0.65 1.70 ± 1.30	0.00 to 3.14/0.17 0.00 to 6.03/1.57	0.50 ± 0.77 2.01 ± 1.90
WSON/WETN	0.00 to 0.40/0.07 0.00 to 0.48/0.16	0.07 ± 0.08 0.14 ± 0.10	0.00 to 0.17/0.02 0.00 to 0.18/0.12	0.05 ± 0.06 0.11 ± 0.07	0.00 to 0.40/0.10 0.00 to 0.22/0.05	0.12 ± 0.10 0.09 ± 0.10	0.00 to 0.17/0.00 0.09 to 0.31/0.14	0.03 ± 0.04 0.16 ± 0.06	0.00 to 0.31/0.06 0.00 to 0.48/0.16	0.07 ± 0.08 0.19 ± 0.12

https://doi.org/10.5194/acp-23-2119-2023 Atmos. Chem. Phys., 23, 2119–2143, 2023

https://doi.org/10.5194/acp-23-2119-2023

Table 1. Continued.

Components	Annual		Summer		Autumn		Winter		Spring	
	Range/med	Avg ± SD	Range/med	Avg ± SD	Range/med	Avg ± SD	Range/med	Avg ± SD	Range/med	Avg ± SD
	ND ($n = 121$) HEP ($n = 40$)		ND ($n = 30$, Jun–Aug) HEP ($n = 10$, Jul)		ND ($n = 30$, Sep–Nov) HEP ($n = 10$, Oct)		ND ($n = 30$, Dec–Feb) HEP ($n = 10$, Jan)		ND ($n = 31$, Mar–May) HEP ($n = 10$, Apr)	
Inorganic ions ($\mu g\,m^{-3}$)										
Cl^-	0.01 to 9.22/0.68 0.04 to 6.83/1.25	1.44 ± 1.80 1.87 ± 1.91	0.02 to 0.13/0.06 0.04 to 0.37/0.08	0.07 ± 0.03 0.14 ± 0.12	0.01 to 4.97/1.36 0.11 to 4.05/1.84	1.46 ± 1.45 1.90 ± 1.07	0.64 to 9.22/3.30 2.70 to 6.83/4.08	3.49 ± 1.94 4.56 ± 1.34	0.07 to 2.22/0.57 0.20 to 2.29/0.80	0.64 ± 0.55 0.87 ± 0.62
SO_4^{2-}	0.50 to 21.6/3.73 1.00 to 15.0/5.44	4.56 ± 3.32 5.93 ± 3.78	1.79 to 8.81/4.43 3.09 to 15.0/9.18	4.42 ± 1.73 9.21 ± 4.63	0.50 to 12.8/4.58 1.00 to 8.57/5.44	4.39 ± 2.91 4.30 ± 2.68	1.21 to 21.6/3.26 2.29 to 12.0/3.79	5.62 ± 5.05 4.93 ± 3.00	0.99 to 9.15/3.13 2.00 to 10.9/5.03	3.55 ± 2.00 5.28 ± 2.77
NO_3^-	0.08 to 37.7/4.69 0.18 to 27.6/6.35	7.38 ± 8.16 8.59 ± 7.57	0.08 to 8.85/0.33 0.18 to 5.59/1.21	0.91 ± 1.65 2.06 ± 1.98	0.13 to 31.8/8.11 1.35 to 27.6/11.0	9.90 ± 9.41 11.4 ± 9.63	2.26 to 37.7/8.38 4.68 to 18.6/9.82	11.1 ± 8.29 10.7 ± 4.66	0.74 to 21.0/4.91 1.91 to 24.5/7.55	6.90 ± 5.85 10.2 ± 8.14
Na^+	0.00 to 0.80/0.11 0.01 to 0.37/0.15	0.15 ± 0.14 0.16 ± 0.09	0.00 to 0.27/0.06 0.11 to 0.22/0.14	0.09 ± 0.06 0.16 ± 0.04	0.01 to 0.38/0.20 0.15 to 0.33/0.23	0.19 ± 0.11 0.23 ± 0.06	0.00 to 0.80/0.22 0.02 to 0.37/0.12	0.27 ± 0.20 0.15 ± 0.11	0.00 to 0.24/0.07 0.01 to 0.25/0.10	0.08 ± 0.07 0.11 ± 0.08
NH_4^+	0.19 to 23.2/3.01 1.06 to 13.1/5.02	4.59 ± 4.12 5.40 ± 3.08	0.62 to 4.72/2.17 1.42 to 5.35/3.93	2.08 ± 0.90 3.67 ± 1.43	0.19 to 18.2/4.48 1.06 to 10.6/5.07	4.97 ± 4.35 4.99 ± 3.46	1.73 to 23.2/5.26 4.09 to 13.1/5.93	6.92 ± 5.05 7.16 ± 2.88	0.97 to 14.5/3.10 1.52 to 11.9/5.48	4.01 ± 2.92 5.79 ± 3.41
K^+	0.03 to 3.83/0.29 0.09 to 1.27/0.39	0.48 ± 0.53 0.49 ± 0.31	0.06 to 0.23/0.12 0.09 to 0.33/0.24	0.13 ± 0.05 0.21 ± 0.09	0.03 to 1.17/0.45 0.24 to 1.05/0.54	0.49 ± 0.36 0.55 ± 0.28	0.16 to 3.83/0.67 0.56 to 1.27/0.79	0.96 ± 0.77 0.84 ± 0.24	0.07 to 0.56/0.27 0.15 to 0.68/0.32	0.29 ± 0.14 0.38 ± 0.19
Mg^{2+}	0.00 to 0.36/0.03 0.00 to 0.15/0.03	0.03 ± 0.04 0.03 ± 0.04	0.00 to 0.06/0.00 0.00 to 0.03/0.03	0.00 ± 0.01 0.00 ± 0.01	0.00 to 0.06/0.00 0.00 to 0.00/0.00	0.01 ± 0.02 0.00 ± 0.00	0.02 to 0.36/0.04 0.04 to 0.15/0.06	0.06 ± 0.07 0.07 ± 0.03	0.00 to 0.06/0.03 0.00 to 0.11/0.03	0.03 ± 0.02 0.04 ± 0.04
Ca^{2+}	0.00 to 0.81/0.13 0.00 to 1.08/0.17	0.11 ± 0.12 0.22 ± 0.23	0.00 to 0.30/0.00 0.00 to 0.41/0.05	0.02 ± 0.06 0.08 ± 0.12	0.00 to 0.32/0.01 0.04 to 0.21/0.10	0.07 ± 0.08 0.11 ± 0.05	0.05 to 0.81/0.15 0.14 to 1.08/0.30	0.20 ± 0.14 0.37 ± 0.26	0.02 to 0.47/0.11 0.01 to 0.85/0.29	0.14 ± 0.11 0.34 ± 0.25
Isotope ratios (‰)										
$\delta^{13}C_{TC}$	−26.5 to −21.9/−25.2	−25.0 ± 0.70	−26.0 to −25.1/−25.6	−25.6 ± 0.26	−25.7 to −21.9/−24.9	−24.7 ± 0.81	−25.9 to −23.7/−24.5	−24.5 ± 0.48	−26.5 to −24.4/−25.4	−25.4 ± 0.53
	−25.5 to −22.8/−24.5	−24.5 ± 0.55	−25.1 to −24.1/−24.8	−24.7 ± 0.30	−24.5 to −22.8/−24.0	−23.9 ± 0.60	−25.1 to −24.1/−24.5	−24.5 ± 0.29	−25.5 to −24.3/−24.9	−24.9 ± 0.34
$\delta^{15}N_{TN}$	1.01 to 22.8/10.2 4.91 to 18.6/9.75	11.4 ± 4.83 10.4 ± 3.43	13.2 to 22.8/17.4 6.86 to 18.6/14.8	17.6 ± 2.52 14.5 ± 3.46	2.93 to 20.2/9.90 5.61 to 12.6/9.49	10.4 ± 4.52 8.78 ± 2.27	1.01 to 11.8/8.86 4.91 to 11.9/8.66	8.21 ± 2.49 8.41 ± 2.12	5.06 to 16.1/9.79 7.01 to 12.2/10.0	9.82 ± 2.72 9.94 ± 1.66
Aerosol mass ($\mu g\,m^{-3}$)										
$PM_{2.5}$	3.38 to 170/23.6 7.56 to 103/38.9	34.9 ± 29.8 43.5 ± 23.8	3.38 to 30.4/13.6 7.56 to 36.6/20.7	13.9 ± 6.24 20.3 ± 9.73	5.02 to 134/33.9 19.3 to 80.1/38.3	39.4 ± 33.0 41.6 ± 21.7	14.1 to 170/42.4 38.9 to 103/54.2	55.1 ± 34.9 62.2 ± 23.2	9.15 to 67.5/23.6 29.2 to 78.5/48.6	28.4 ± 14.5 49.8 ± 17.8

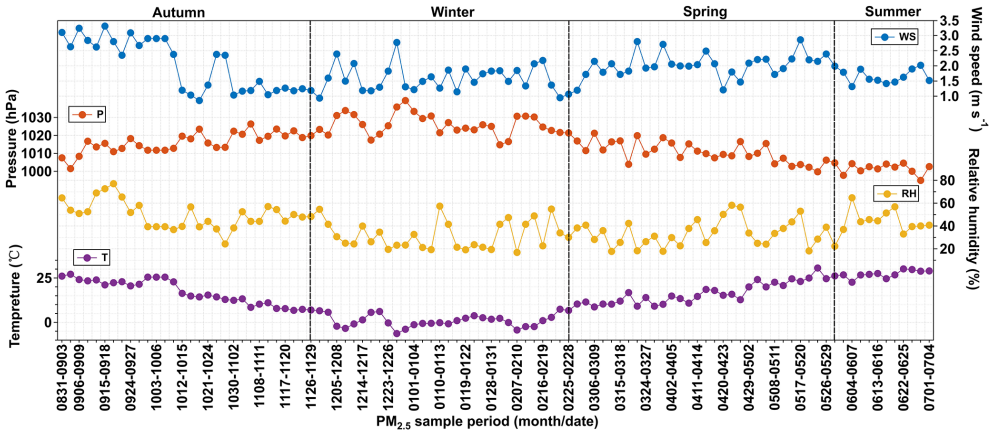

Figure 2. Temporal variations of ambient temperature (T), atmospheric pressure (P), wind speed (WS) and relative humidity (RH) in Tianjin from September 2018 to July 2019.

forcement of the control and prevention measures on pollutant emissions from various sources to improve the air quality further in this region.

3.3 Concentrations and seasonal variations of carbonaceous components

On average, the OC accounted for 17.3 % in $PM_{2.5}$ mass at ND and 13.3 % at HEP in Tianjin. The relative abundance of WSOC in OC was found to be 71.1 ± 14.5 % at ND and 65.6 ± 16.8 % at HEP. The average concentration of SOC was $3.11 \pm 3.42\,\mu g\,m^{-3}$ at ND and $3.76 \pm 3.44\,\mu g\,m^{-3}$ at HEP, accounting for 53.3 % and 57.5 % in OC, respectively. OC, WSOC and SOC showed clear seasonal changes during the campaign (Fig. 4). At ND, the average concentrations of OC and WSOC were higher in winter than in autumn, followed by spring and summer. On average, OC was 4 times higher in winter than that in summer at both ND and HEP. However, the average concentration of EC in winter was only about 1.7 times compared to that in summer at ND and 1.3 times at HEP. The higher loading of OC compared to that of EC in winter indicates that the OC emission from coal/biomass combustion should have been higher rather than EC in winter. In addition, the secondary formation of OC might be significant via adsorption and/or NO_3 radical-driven oxidation reactions of VOCs (G. Wang et al., 2016; Robinson et al., 2007). On the other hand, the temperate continental climate prevails over the Tianjin region, and the East Asian monsoon brings the humid oceanic air masses during summer that result in frequent precipitation events, which might cause the enhanced wet deposition of pollutants, including EC in summer (Y. Wang et al., 2016b; Luo et al., 2018; Tao et al., 2014). Interestingly, the average concentration of SOC in winter ($6.78\,\mu g\,m^{-3}$, ND; $8.68\,\mu g\,m^{-3}$, HEP) was found to be 6 times higher than that in summer ($1.08\,\mu g\,m^{-3}$, ND; $1.18\,\mu g\,m^{-3}$, HEP), which indicates that the formation of SOC was highly significant in the Tianjin atmosphere during winter. The average WSOC was 0.69–16.0 at ND and 0.66–9.44 $\mu g\,m^{-3}$ at HEP. Such a higher level of WSOC at ND compared to that at HEP indicates its higher emission (potentially from biomass burning) and/or secondary formation under a high abundance of oxidants at ND than that at HEP.

3.4 Implications for $PM_{2.5}$ sources through relationships and mass ratios of carbonaceous components

Generally, EC does not react at ambient temperature and remains relatively stable in the atmosphere, and hence it is often used as a tracer for primary pollutants. Therefore, the scatter plots between EC and OC and their mass ratios can provide insights in tracing the origins of atmospheric aerosols and the extent of secondary formation of OC in the atmosphere. As shown in Fig. 5, OC showed a moderate correlation with EC in $PM_{2.5}$ at ND in spring ($R^2 = 0.45$, $p < 0.05$), summer ($R^2 = 0.50$, $p < 0.05$) and winter ($R^2 = 0.54$, $p < 0.05$) but a weak correlation ($R^2 = 0.05$, $p < 0.05$) in autumn. Such linear relations suggest that both OC and EC might have been derived from similar sources in spring, summer and winter at ND, whereas their sources might be different in autumn. The slope value was found to be higher in winter, which indicates that the contribution of OC from primary sources was higher in winter than in the other seasons. However, at HEP, the correlation between OC and EC in $PM_{2.5}$ in spring, summer, autumn as well as winter was very poor (Fig. 5), which implies that the sources of OC and EC were significantly different at HEP. Such differences between ND and HEP suggest that possible emissions of biogenic VOCs from rich vegetation including agricultural plants and/or biomass burning might be high at HEP and in the surrounding areas, and those VOCs must be subjected to in situ photochemical oxidation, resulting in high loading of OC compared to that of EC. As can be seen from Fig. 5d–e, $PM_{2.5}$ showed a high correlation with OC in autumn, winter

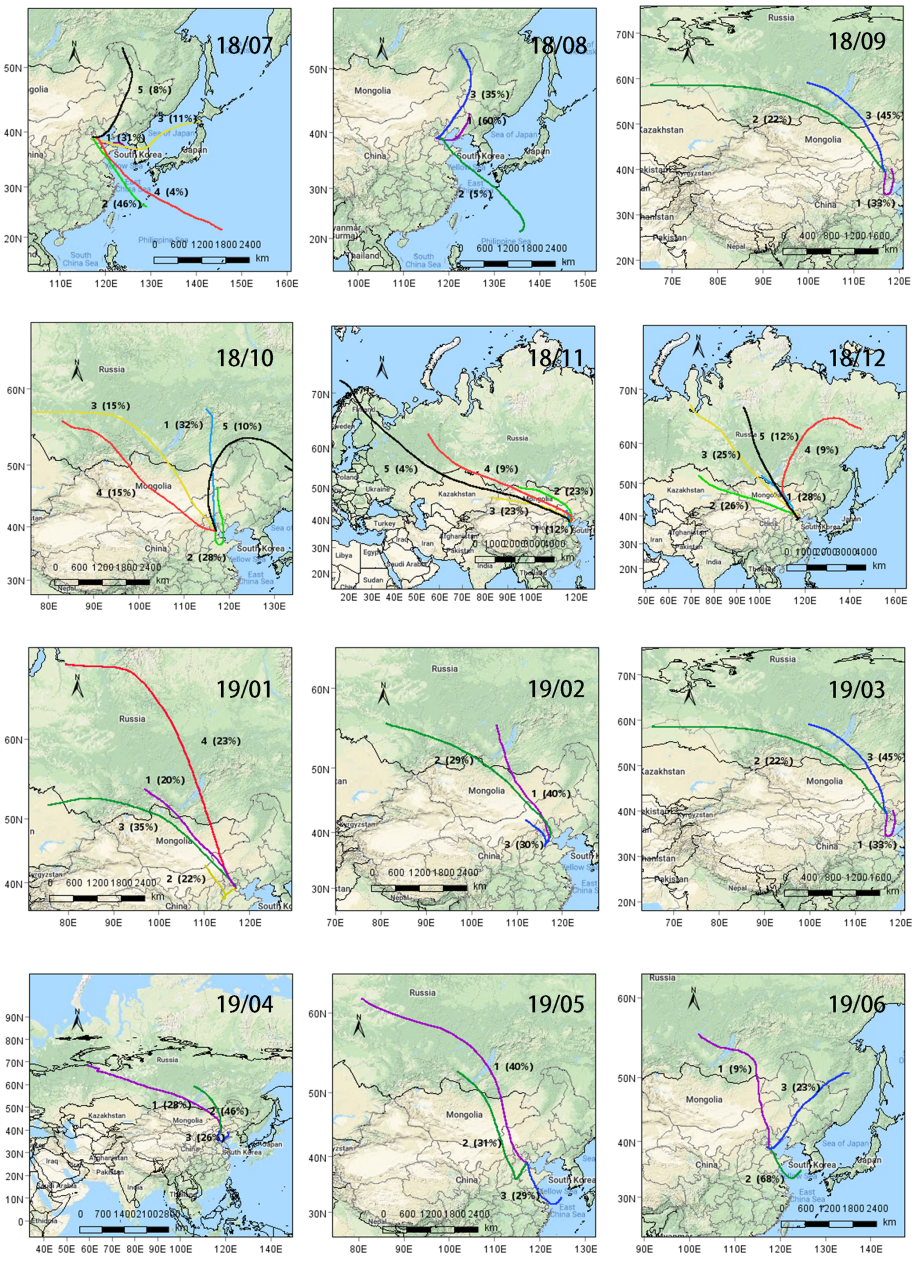

Figure 3. Monthly cluster analysis plots of 5 d backward air mass trajectories arriving over Tianjin at 500 m a.g.l. during the campaign period. (The maps were generated by the MeteoInfo software using © Google Maps.)

and spring at both the sampling points but a very poor correlation with EC, except in summer at HEP, which indicates that the loading of $PM_{2.5}$ was mainly driven by the OC loading. However, at HEP, the $PM_{2.5}$ showed a good correlation with EC in winter (Fig. 5e), indicating that the contribution from the primary sources was also important at HEP in winter.

Generally, the OC/EC ratio in the atmosphere is used to identify the emission and transformation characteristics of carbon particles. Chow et al. (2007) reported that when the OC/EC is higher than 2.0, it could be considered that the secondary formation of OC in the atmosphere is significant. On the other hand, the OC/EC varies significantly depending on their relative contributions from the emissions of coal combustion (range: 8.1–12.7), vehicle exhaust (0.7–2.4), biomass burning (4.1–14.5), wood combustion (16.8–40.0) and cooking (32.9–81.6) (Watson et al., 2001). The OC/EC ratios were 6.56–48.1 at ND and 4.01–63.0 at HEP, which are close to those reported for the particles emitted from biomass burning, including wood combustion and coal combustion, but not those from diesel and gasoline-driven vehicle exhaust.

Table 2. $PM_{2.5}$ mass concentrations in Tianjin and those reported at other different locales in China and around the world.

City/nation	Sampling period	$PM_{2.5}$ ($\mu g\,m^{-3}$)	Reference
Tianjin, North China (urban site)	2018–2019	34.9 ± 29.7	This study
Tianjin, North China (suburban petrochemical industrial site)	2018–2019	43.47 ± 23.5	This study
Zibo, North China	2006–2007	164.61 ± 79.14	Luo et al. (2018)
Beijing, North China	2009–2010	135.0	Zhang et al. (2013)
Beijing, North China	2013	84	Xu and Zhang (2020)
Beijing, North China	2018	50	Xu and Zhang (2020)
Tianjin, North China	2008	109.8	Gu et al. (2010)
Harbin, Northeast China	2017	59.39 ± 46.9	Chen et al. (2019)
Chengdu, Southeast China	2017	56.3 ± 28.1	Huang et al. (2018)
Chengdu, Southeast China	2014–2015	67.0 ± 43.4	Wang et al. (2018)
Chengdu, Southeast China	2011	119 ± 56	Tao et al. (2014)
Ningbo, coastal Southeast China	2012–2013	42.4	M. Li et al. (2017)
Nanjing, coastal Southeast China	2013–2014	129	Li et al. (2016)
Guangzhou, South China	2012-2013	44.2	Lai et al. (2016)
Shanghai, coastal Southeast China	2011–2012	68.4	Zhao et al. (2015)
Los Angeles, USA	2005–2006	19.88	Hasheminassab et al. (2014)
Atlanta–Yorkville, USA	2001–2005	14.3	Chen et al. (2012)

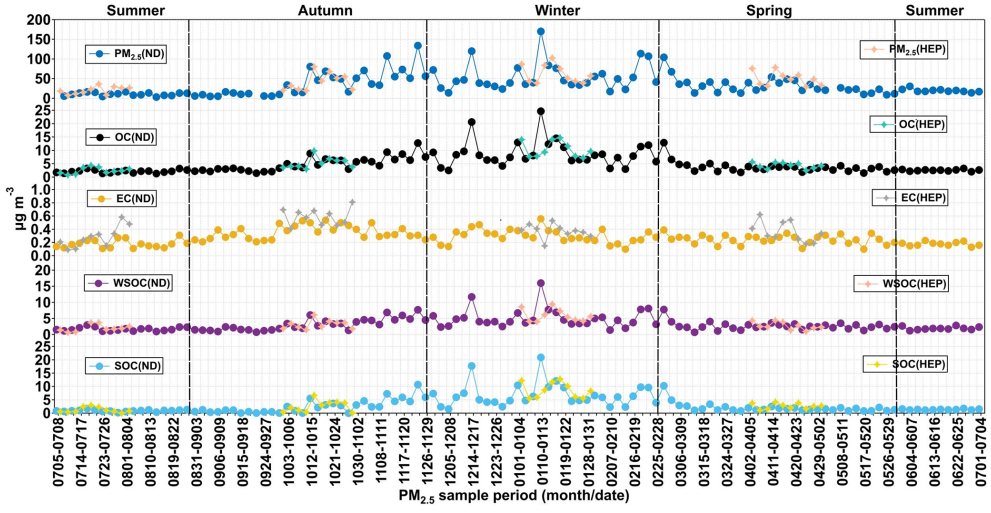

Figure 4. Temporal variations in concentrations ($\mu g\,m^{-3}$) of $PM_{2.5}$ and its chemical components OC, EC, WSOC and SOC at ND (solid dots) and HEP (solid stars) in Tianjin during 2018–2019. See the text for abbreviations.

The average OC/EC was 17.8 at ND and 15.7 at HEP, which are 8.7 and 7.8 times higher than 2.0, which indicates that the significant secondary formation of OA over the Tianjin region was significant. It has been reported that the ambient OC/EC in aerosols was gradually increasing over the period from 2000 to 2010 in China, confirming the increase in OC that should have been produced by enhanced oxidation in the atmosphere rather than from primary emissions (Cui et al., 2015). The high OC/EC ratios in the atmosphere of Tianjin once again demonstrated the enhanced emission and/or secondary formation of OC in China. On the other hand, the OC/EC ratio in winter was significantly higher than that in other seasons, especially at HEP, despite the fact that it is a suburban area (Fig. 6). Therefore, the increase in OC/EC in winter can be attributed to the increase in emission of VOCs from coal combustion due to its enhanced consumption for domestic heating and subsequent secondary formation of OC under stagnant weather conditions.

WSOC is mainly generated by oxidation reactions of VOCs in the atmosphere in addition to primary emissions such as biomass burning, and hence the mass fraction of WSOC in OC has been considered to be an indicator of aging of aerosols in the atmosphere, when the contribution of the WSOC is relatively low or insignificant from the biomass burning emission (Aggarwal and Kawamura, 2009). As shown in Fig. 5f, the correlation between $PM_{2.5}$ and

WSOC was much lower in summer than that in other seasons, which indicates that the secondary formation of the WSOC was more important than its primary emission, particularly in summer. Interestingly, WSOC/OC in Tianjin aerosols was found to be higher in spring and summer than in winter and autumn at both sites (Fig. 6). Such a high abundance of WSOC indicates the enhanced secondary formation of OC in spring and summer rather than in autumn and winter, because the biomass/biofuel combustion is significantly lower and because the VOC emissions from marine and terrestrial biota including croplands and subsequent photochemical processing are intensive in the gas and/or aqueous phases in spring/-summer (Padhy and Varshney, 2005; Pavuluri et al., 2013) compared to that in autumn/winter. In fact, being a coastal city, Tianjin receives marine air masses that are enriched with marine biological emissions due to the occurrence of sea breeze during daytime that are subjected to subsequent photochemical oxidation in the atmosphere. In addition, the air masses arriving in Tianjin during summer originated from the oceanic region (Fig. 3) and were also enriched with marine biological emissions and aged during the long-range atmospheric transport. On the other hand, the range and average WSOC/OC in Tianjin aerosols at ND and HEP (Table 1) are similar to those reported at urban locations, Nanjing, China (0.40–0.51) (Yang et al., 2005), and Chennai, India (0.23–0.61) (Pavuluri et al., 2011), and in largely rural areas of Hungary (range 0.38–0.72, average 0.66) (Kiss et al., 2002), where biomass burning was considered to be the major source of aerosols and aged during long-range atmospheric transport. Furthermore, WSOC and OC showed a very good linear relationship at both sites in all the seasons, which indicates that the contribution of OA from biomass burning emissions was also significant in addition to the secondary formation and/or transformations, particularly in autumn and winter, in the Tianjin region.

Interestingly, SOC/OC ratios were found to be higher in winter, followed by spring, summer and autumn (Table 1). The higher loading of SOC in winter might have occurred due to enhanced absorption/adsorption of VOCs to existing particles. In addition, despite lower temperatures prevailing over the Tianjin region, the secondary formation of OA might be intensive in winter by NO_3 radical reactions. It has been reported that the haze formation in China is mainly driven by the enhanced secondary formation of aerosols by NO_3 radical reactions (J. Wang et al., 2016). In fact, average concentrations of NO_2 that can be oxidized to NO_3 radicals by O_3 (Brown and Stutz, 2012) were significantly higher in winter (54.4 $\mu g\,m^{-3}$), followed by autumn (52.3 $\mu g\,m^{-3}$) and spring (39.1 $\mu g\,m^{-3}$), and lower in summer (30.3 $\mu g\,m^{-3}$) in the Tianjin atmosphere during the campaign (Li et al., 2021). Such higher levels of NO_2 might substantially be transformed to NO_3 radicals and accelerate the oxidation of VOCs of mostly biogenic origin, preferably through unimolecular reactions (Draper et al., 2019; Ng et al., 2017), and thus promote the formation of SOA, including organic nitrates, which may not be fully water-soluble. In fact, the average concentration of WSOC was higher than that of SOC in spring, summer and autumn but opposite in winter (Table 1). Such differences indicate that the SOC produced in spring, summer and autumn might be mostly water-soluble, whereas in winter, part of the SOC is water-insoluble. In fact, WIOC accounts for 41.8 % of OC in winter at ND and 43.2 % at HEP, suggesting that part of the SOC (e.g., N-containing organics) might be water-insoluble. However, the temporal trends of WIOC, SOC and WSOC were similar, which implies that they should have originated from the same/similar sources and that their formation processes might also be similar in each season over the Tianjin region.

Furthermore, SOC showed a strong correlation with WIOC at both ND and HEP ($R^2 = 0.86$, $p < 0.05$ and 0.67, $p < 0.05$), and their slope values were significantly higher in winter but not in summer ($R^2 = 0.05$, $p < 0.05$ and 0.00, $p < 0.05$; Fig. 5). Such differences clearly imply that the secondary formation and/or transformation processes were quite different in winter from those in summer, and most of the SOC generated in winter was water-insoluble. Simulations, field observations, and laboratory studies have shown that the secondary formation of OA in the atmosphere over China is enhanced in winter, and only the aqueous-phase secondary formation has been considered the prominent pathway (Huang et al., 2014; J. Wang et al., 2016). Therefore, the enhanced formation of SOC in Tianjin aerosols, including WIOC, warrants further investigation of the possible formation processes of the WIOC, particularly in winter under the high abundance of NO_3, a subject of further research.

3.5 Implications for $PM_{2.5}$ sources through $\delta^{13}C_{TC}$

The box-and-whisker plots of seasons and annual $\delta^{13}C_{TC}$ and $\delta^{15}N_{TN}$ in Tianjin aerosols are depicted in Fig. 7. The $\delta^{13}C_{TC}$ was −26.5 ‰ to −21.9 ‰ with an average of -25.0 ± 0.7 ‰ at ND (Table 1). They showed a temporal trend with a gradual enrichment of ^{13}C in autumn and winter followed by a gradual depletion in the ^{13}C to early summer and remained stable thereafter, except for a few cases at ND (Fig. 8), while at HEP, $\delta^{13}C_{TC}$ −25.5 ‰ to −22.8 ‰ (average -24.5 ± 0.55 ‰) during the campaign period and their seasonal variations were similar to those found at ND, which indicates that the Tianjin aerosols should have been significantly derived from different sources in different seasons. The decreasing trend of $\delta^{13}C_{TC}$ from late winter to early summer through spring confirms the important role of biological emissions, because the VOCs and unsaturated fatty acids emitted from higher plants are depleted in ^{13}C, as evidenced by the $\delta^{13}C$ of fatty acids in unburned C_3 vegetation (range: −38.5 % to −32.4 %) (Ballentine et al., 1998). In summer, the stability of $\delta^{13}C_{TC}$ might have been controlled by significant aging of OA under high solar radiation through enhanced photochemical reactions, which simultaneously led to the enrichment of ^{13}C in reactants and

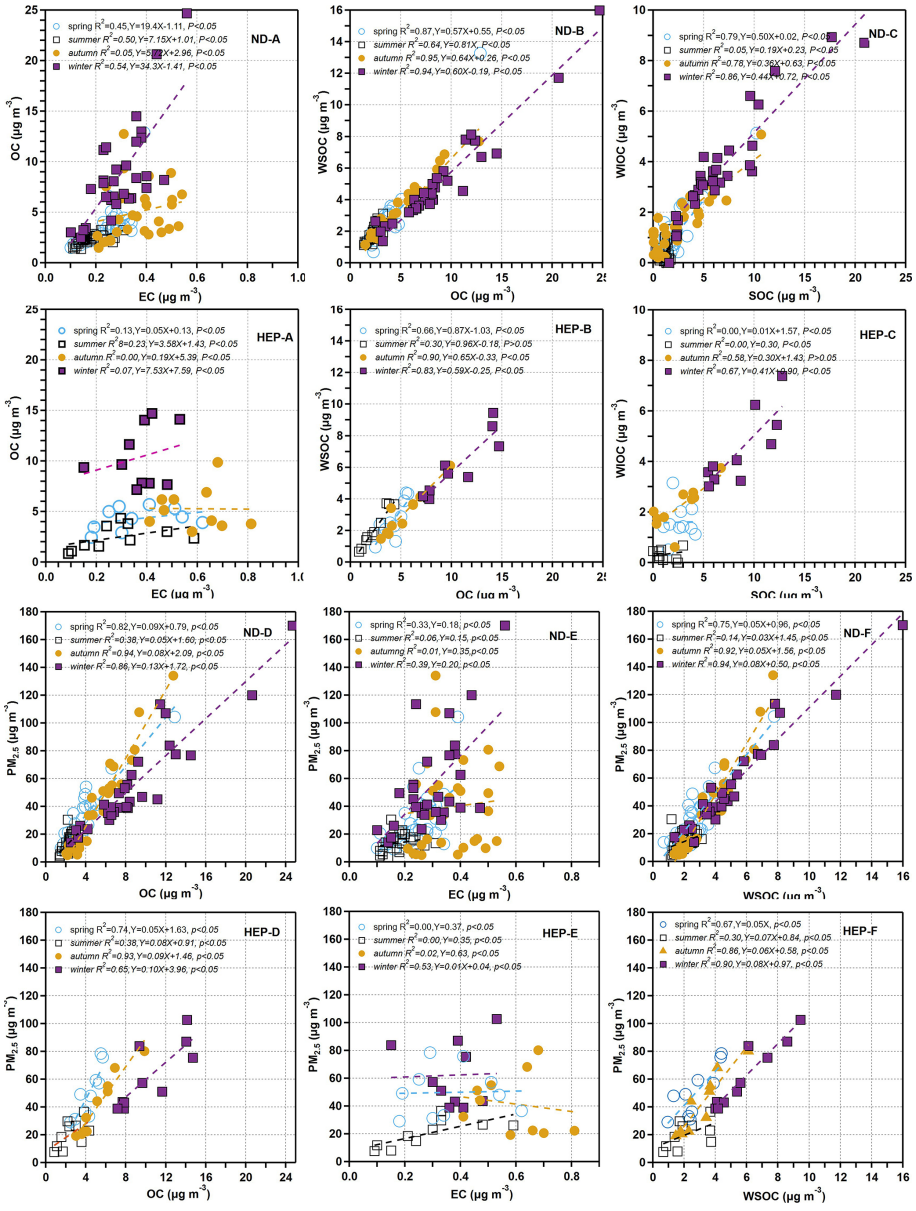

Figure 5. Scatter plots of selected carbonaceous components in $PM_{2.5}$ in Tianjin at ND and HEP.

its depletion in product compounds. The increasing trend of $\delta^{13}C_{TC}$ in autumn and winter indicates that the contribution of carbonaceous aerosols from biomass burning and fossil fuel combustion was large. The enrichment of ^{13}C occurred in particles produced by biomass burning, while the $\delta^{13}C$ of aerosol carbon produced by fossil fuel combustion was relatively higher than that of aerosol carbon produced by biological sources. In fact, the consumption of fossil fuels for heating in winter in Tianjin is much higher than in other seasons.

Figure 9 shows the $\delta^{13}C_{TC}$ of the particles emitted from point sources and/or source materials reported in the literature together with those found in Tianjin aerosols at both ND and HEP. The average $\delta^{13}C_{TC}$ at ND was comparable to that reported for total suspended particles (TSPs) over the western South China Sea (SCS), which were considered to be significantly influenced by biomass burning emissions, especially C_3 plants (Song et al., 2018). They were also comparable to those reported in aerosols (fine mode ($D_P < 2\,\mu m$) and PM_{10}) in the Santarem region and in Mumbai, India, where biomass/biofuel burning emissions were expected to be the major sources of carbonaceous aerosols (Martinelli et al., 2002; Pavuluri et al., 2015c). Furthermore, the average $\delta^{13}C_{TC}$ in HEP aerosols was similar to that reported in TSPs from Mount Tai in early June, which was considered to be highly influenced by burning activities of crop residues in

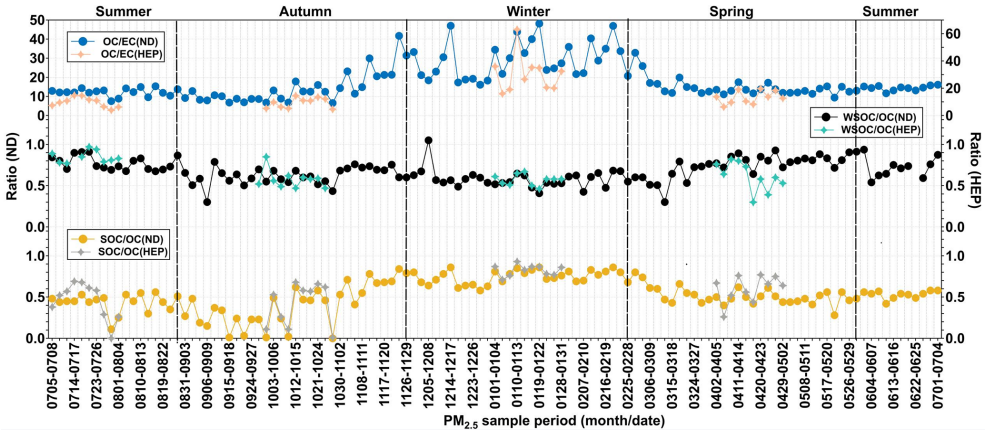

Figure 6. Temporal variations in the ratios of OC/EC, WSOC/OC and SOC/OC in $PM_{2.5}$ at ND and HEP in Tianjin during 2018–2019. See the text for abbreviations.

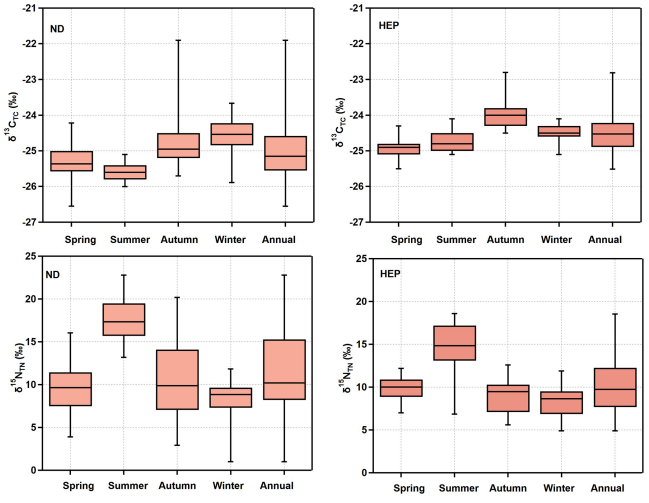

Figure 7. Box-and-whisker plot of seasonal variations in stable carbon and nitrogen isotope ratios of total carbon ($\delta^{13}C_{TC}$) and nitrogen ($\delta^{15}N_{TN}$) in $PM_{2.5}$ at ND and HEP in Tianjin during the campaign. The cross bar in the box shows the median, and the open circles show the outliers.

the North China Plain (Fu et al., 2012). Pavuluri and Kawamura (2017) reported a similar $\delta^{13}C_{TC}$ (-24.8 ± 0.68 ‰) in TSPs in Sapporo, which were also strongly influenced by biomass burning and fossil fuel combustion emissions. Such comparisons clearly imply that the biomass burning emissions are the major sources of atmospheric aerosols in the Tianjin region, although we do not preclude the importance of other sources.

3.6 Concentrations and seasonal variations of nitrogenous components and other inorganic ions

Concentrations of the measured water-soluble inorganic ions showed the high abundance of NO_3^- at both the sites, followed by $NH_4^+ > SO_4^{2-} > Cl^- > K^+ > Na^+ > Ca^{2+} > Mg^{2+}$ at ND and $SO_4^{2-} > NH_4^+ > Cl^- > K^+ > Ca^{2+} > Na^+ > Mg^{2+}$ at HEP in Tianjin. Averages of the sums of ions were $18.7 \pm 16.9\,\mu g\,m^{-3}$ and $22.7 \pm 13.1\,\mu g\,m^{-3}$ (Table 1), accounting for 55 % of the $PM_{2.5}$ mass at ND and 56 % at HEP. SO_4^{2-}, NO_3^- and NH_4^+ were found to be the major ions, and their total concentrations accounted for 89 % in the total concentration of the measured ions at ND and 87 % at HEP. Among them, SO_4^{2-}, NO_3^- and NH_4^+ were 33 %, 31 % and 25 %, respectively, at ND and 29 %, 33 % and 24 %, respectively, at HEP. The concentration of NO_3^- was the highest, accounting for 17 % of the $PM_{2.5}$ mass at ND and 18 % at HEP.

As can be seen from Fig. 10, the concentration of NO_3^- peaked in winter and was lower in summer. In addition to primary emissions contributing a large amount of NO_3^- in winter, it is likely because the low temperatures in winter promote the partitioning of NO_3^- from the gas to particulate phases, whereas in summer, the higher temperatures enhance the transformation of NH_4NO_3 to HNO_3 (Utsunomiya and Wakamatsu, 1996), and the frequent precipitation might cause the wet deposition of the NO_3^-. The highest concentration of SO_4^{2-} appeared in winter and the lowest in spring (Table 1). In winter, SO_2 emission is significantly increased due to the high consumption of fossil fuel, including coal combustion for domestic heating in the northern parts of China. The higher concentration of SO_4^{2-} in summer than in spring might be due to higher temperature, relative humidity and abundant sunlight, which provide favorable conditions for the photochemical conversion of SO_2 to SO_4^{2-} through gas- and aqueous-phase reactions. In addition, the air mass from the ocean in summer brings abundant SO_4^{2-} from the perspective of emission sources. Interestingly, the seasonal variations of SO_4^{2-} at HEP were quite different from those at ND, with the highest in summer and the lowest in autumn.

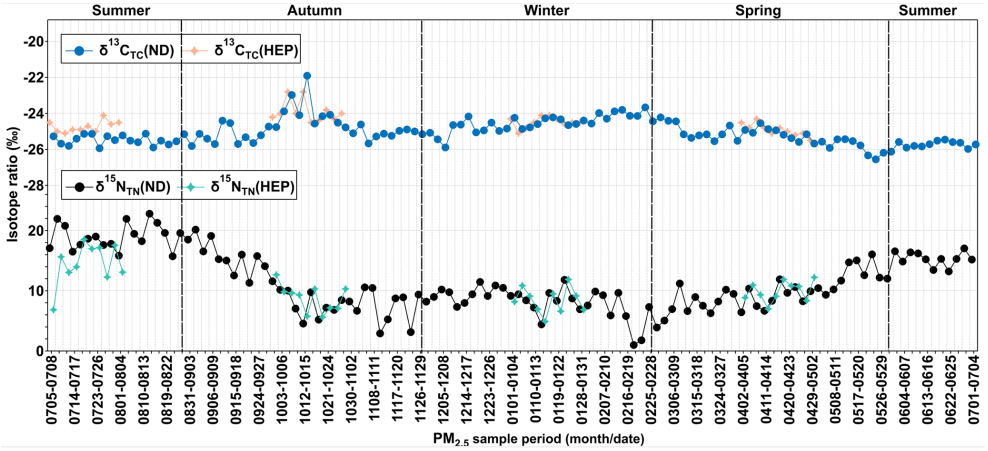

Figure 8. Temporal variations in $\delta^{13}C_{TC}$ and $\delta^{15}N_{TN}$ in $PM_{2.5}$ at ND (solid dots) and HEP (solid stars) in Tianjin during the campaign period (2018–2019).

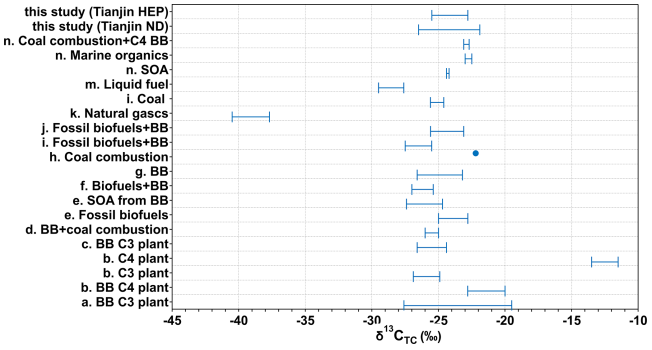

Figure 9. Range or mean $\delta^{13}C_{TC}$ in the particles emitted from point sources, source substances and atmospheric aerosols from different sites around the world. **(a)** Cao et al. (2016); **(b)** Martinelli et al. (2002); **(c)** Song et al. (2018); **(d)** Garbaras et al. (2015); **(e)** Bikkina et al. (2016); **(f)** Aggarwal et al. (2013); **(g)** Fu et al. (2012); **(h)** Kunwar et al. (2016); **(i)** Cachier et al. (1986); **(j)** Pavuluri and Kawamura (2016); **(k, l, m)** Widory (2007); **(n)** Kundu et al. (2014).

In addition, the loading of SO_4^{2-} was always higher at HEP than at ND. In fact, as noted earlier, HEP was much closer to the seashore, and the aerosol composition must be more influenced by sea breeze during daytime throughout the year (Bei et al., 2018), while in summer, the air masses originated from the oceanic region that should have been enriched with marine biogenic emissions including dimethyl sulfide (DMS), which converts to SO_2 and then SO_4^{2-} upon photochemical oxidation (Yan et al., 2020). On the other hand, the industries including petrochemical processing units are located near the seashore, and their emissions including SO_2 might have a significant impact on the aerosol composition at HEP, whereas at ND, local anthropogenic emissions, e.g., automobile exhausts, might have a greater influence on the composition of $PM_{2.5}$.

Since WSTN is mainly composed of IN ($\Sigma NO_3^- - N + NH_4^+ - N$), the temporal trend of WSTN was found to be similar to that of IN (Fig. 11). Average concentrations of WSTN and IN were high at ND from mid-autumn to winter, and the IN peaked in mid-winter, whereas WSON peaked in late autumn. In addition, the average concentration of WSON was higher in autumn, followed by spring, winter and summer. On average, the mass fraction of WSON in WSTN was 6.74 ± 7.81 % (range 0 %–39.5 %). At HEP, the average concentration of WSTN was $7.34 \pm 5.13\,\mu g\,m^{-3}$, and IN was $6.14 \pm 3.90\,\mu g\,m^{-3}$ (Table 1). Their average concentrations showed a seasonal pattern with higher levels in winter followed by spring and autumn, and the WSTN peaked in winter, whereas IN peaked in spring. In addition, the concentration of WSON was higher ($2.01 \pm 1.80\,\mu g\,m^{-3}$) in the growing season than that in winter and autumn.

3.7 Implications for $PM_{2.5}$ sources through mass ratios and relationships of nitrogenous components and other inorganic ions

The mass ratio of NO_3^- to SO_4^{2-} reflects the relative contribution from local moving sources (motor vehicles) and fixed sources (including coal combustion) to atmospheric aerosols. Generally, if the ratio is ≥ 1, automobile exhaust is considered to be an important source of the particles in the given environment (Ming et al., 2017). The NO_3^-/SO_4^{2-} ratio was found to be higher than 1 in all the seasons, except for summer (0.21), and the annual average was 1.63 at ND, which indicates that the automobile exhaust was also an important source of the $PM_{2.5}$ in the urban area of Tianjin. In summer, the air masses originating from the oceanic region should have been enriched with the marine biogenic emissions including DMS, and thus the contribution of biogenic SO_4^{2-} might be significant in Tianjin aerosol. The NO_3^-/SO_4^{2-} in Tianjin (ND: 1.63, HEP: 1.35) is similar to that reported in

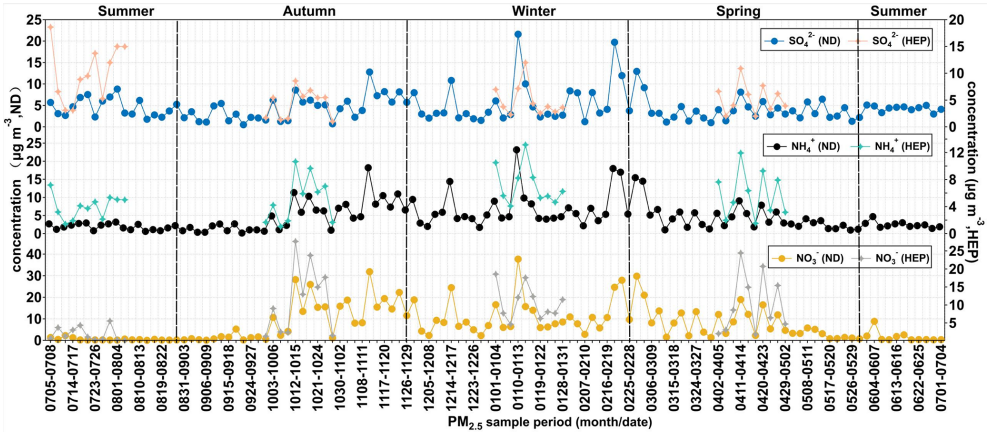

Figure 10. Temporal variations in concentrations (μg m^{-3}) of secondary ionic species in $PM_{2.5}$ at ND (solid dots) and HEP (solid stars) in Tianjin during the campaign period (2018–2019).

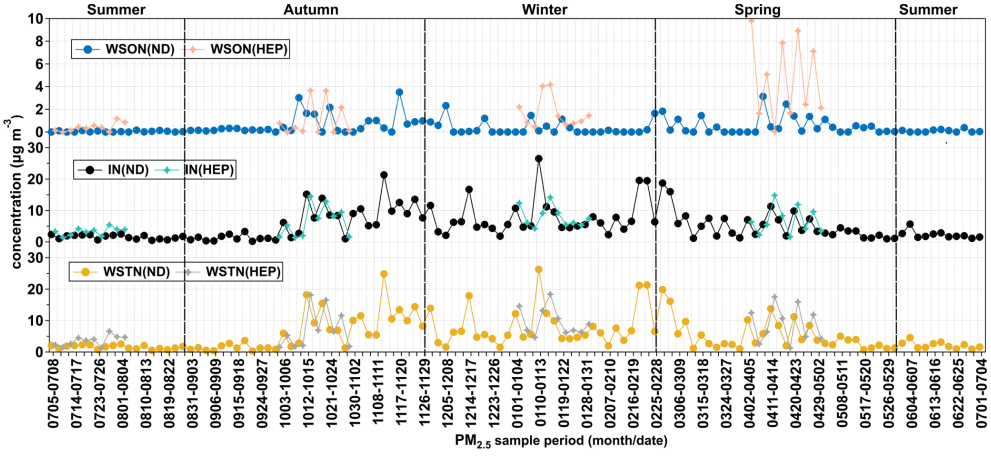

Figure 11. Temporal variations in WSTN, IN and WSON (μg m^{-3}) in $PM_{2.5}$ at ND (solid dots) and HEP (solid stars) in Tianjin during the campaign period (2018–2019).

Beijing (1.37) (Xu et al., 2017) and Shanghai (1.05), where automobile exhausts have been considered one of the major sources. Such comparability again supports our finding that automobile exhausts are an important source of aerosols in Tianjin.

The correlation between SO_4^{2-} and NO_3^- was good in spring ($R^2 \geq 0.55$, $p = 0.08$), autumn and winter ($R^2 \geq 0.55$, $p < 0.05$) but not in summer ($R^2 = 0.00$, $p < 0.05$ at ND and 0.06, $p < 0.05$ at HEP). Such comparability might appear to be due to high emissions of NO_x and SO_2 from fossil fuel, including coal combustion during the cold period (late autumn to the following early spring) and subsequent secondary formation, whereas in summer, the emission of SO_2 from coal combustion in the industrial sector and marine biogenic emission of DMS might be larger than in other seasons. In addition, the NH_4NO_3 is more susceptible to the decomposition into gaseous HNO_3 and NH_3 at higher temperatures (Russell et al., 1983) that prevailed in summer. The annual average concentration of Cl^- was 1.45 ± 1.79 μg m^{-3}, accounting for 4.15 % of the $PM_{2.5}$ mass at ND with the higher loading in winter than in the other seasons. Such a high loading again confirms the enhanced consumption of coal in winter for domestic heating, because the emission of Cl^- is abundant from coal combustion (Zhang et al., 2017; He et al., 2001), while K^+ was also found to be higher in winter, followed by autumn, spring and summer (Table 1). The high loading of K^+ in winter might be due to enhanced biomass burning for domestic heating.

SO_4^{2-} and NO_3^- showed a good correlation with NH_4^+ at ND and moderate and good correlations at HEP but weak or no correlation with alkali (Na^+, Ca^{2+} and Mg^{2+}) ions at both sites (Table 3), suggesting that they were mainly associated with NH_4^+ in the form of $(NH_4)_2SO_4/NH_4HSO_4$ and NH_4NO_3 rather than with alkali metals. Interestingly, the SO_4^{2-}, NO_3^- and NH_4^+ showed a medium correlation with K^+, except for SO_4^{2-} at HEP, which suggests that SO_4^{2-},

Table 3. Correlation coefficients (R^2) of inorganic ions in $PM_{2.5}$ at ND (right) and HEP (left) in Tianjin, North China.

	$PM_{2.5}$	Cl^-	SO_4^{2-}	NO_3^-	Na^+	NH_4^+	K^+	Mg^{2+}	Ca^{2+}
$PM_{2.5}$		0.71	0.63	0.86	0.29	0.90	0.64	0.22	0.26
Cl^-	0.43		0.31	0.56	0.40	0.62	0.67	0.27	0.24
SO_4^{2-}	0.05	0.03		0.54	0.10	0.74	0.46	0.16	0.09
NO_3^-	0.57	0.21	0.03		0.21	0.92	0.49	0.11	0.15
Na^+	0.17	0.07	0.09	0.13		0.21	0.20	0.05	0.19
NH_4^+	0.80	0.30	0.24	0.71	0.18		0.56	0.15	0.16
K^+	0.64	0.71	0.00	0.47	0.19	0.55		0.66	0.24
Mg^{2+}	0.36	0.30	0.00	0.04	0.02	0.21	0.27		0.45
Ca^{2+}	0.38	0.13	0.01	0.07	0.06	0.25	0.18	0.81	

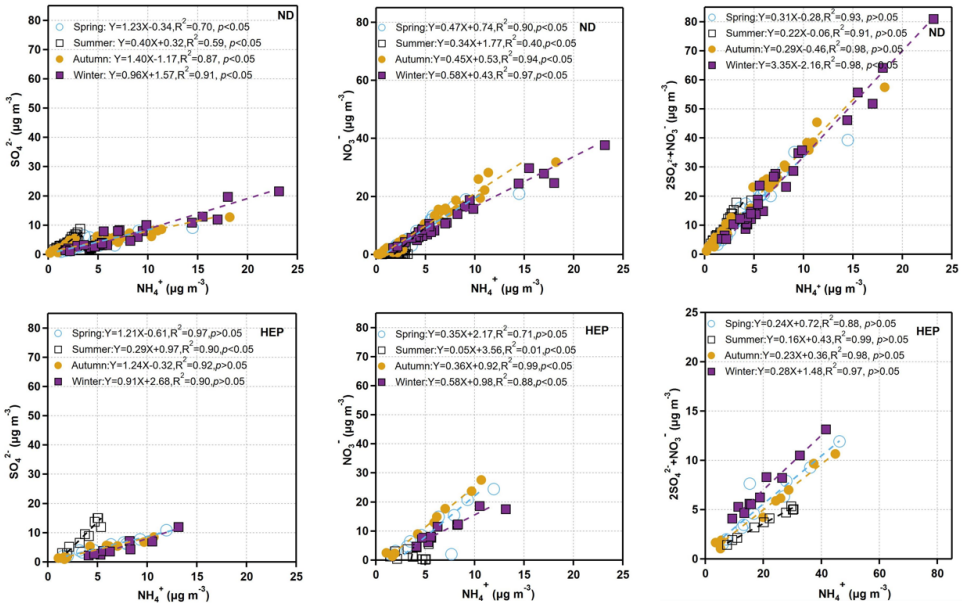

Figure 12. Linear relations between secondary ions in $PM_{2.5}$ at ND and HEP in Tianjin during the campaign period.

NO_3^- and NH_4^+ might have been significantly derived from biomass burning emissions. The nonexistent correlation between K^+ and SO_4^{2-} indicates that the sources of SO_4^{2-} were significantly different from those of NH_4^+, NO_3^- and K^+ at HEP. As discussed in the previous section, the SO_4^{2-} might have been significantly derived from industrial emissions, particularly from petrochemical plants that existed near HEP, and/or a larger contribution of SO_4^{2-} derived from marine biogenic emissions due to sea breeze. The correlation coefficient between Ca^{2+} and Mg^{2+} was relatively high (Table 3), which indicates that they might have been emitted from the same source such as soil dust. However, the mass ratio of Mg^{2+} to Ca^{2+} was 0.27 at ND and 0.14 at HEP, which is comparable to those reported at the point source of coal combustion (Wang et al., 2005), implying that the Ca^{2+} and Mg^{2+} in Tianjin aerosols are derived not only from soil dust, but also from coal combustion emissions.

The molar ratios of NH_4^+/SO_4^{2-}, NH_4^+/NO_3^- and $NH_4^+/(2SO_4^{2-}+NO_3^-)$ can indicate their coexistence forms (Lyu et al., 2015; Behera et al., 2013). Figure 12 shows the linear relations between NH_4^+ and SO_4^{2-}, NO_3^- and $(2SO_4^{2-}+NO_3^-)$. NH_4^+ showed significant correlations with SO_4^{2-} and NO_3^- except for summer, confirming that sufficient NH_3 was present to neutralize H_2SO_4 and HNO_3 during the campaign period. The relatively higher correlation of NH_4^+ with NO_3^- than that with SO_4^{2-} suggests that NH_4NO_3 might be more likely formed than $(NH_4)_2SO_4$ because of a better affinity between the two ions (Blanchard and Hidy, 2003) at both sites (Table 3). Furthermore, the slopes and coefficients between the selected ions (Fig. 12) indicated that NH_4NO_3, $(NH_4)_2SO_4$, NH_4HSO_4 and NH_4NO_3 were the more likely existing forms of secondary inorganic ions in Tianjin in all seasons, except for summer, during which the $(NH_4)_2SO_4$

might have existed due to the loss of HNO_3 and enhancement of NH_3 emissions at high temperatures.

3.8 Implications for $PM_{2.5}$ sources through $\delta^{15}N_{TN}$

$\delta^{15}N_{TN}$ was 1.10 ‰–22.8 ‰ (11.4 ± 4.8 ‰) at ND and 4.91 ‰–18.6 ‰ (10.4 ± 3.4 ‰) at HEP during the campaign. The temporal trends at ND and HEP were highly comparable with each other (Fig. 7). The averages of $\delta^{15}N$ varied significantly from season to season, with higher values in summer (17.7 ± 2.51 ‰ at ND and 14.5 ± 3.3 ‰ at HEP) and lower values (8.07 ± 2.5 ‰ at ND and 8.41 ± 2.0 ‰ at HEP) in winter. Such seasonal changes in $\delta^{15}N_{TN}$ suggest that the aerosol N was significantly influenced by season-specific source(s) and/or the chemical aging of N species.

The range (or average) of $\delta^{15}N$ reported for the particles emitted from point sources as well as those reported in atmospheric aerosols from different locations over the world together with those obtained in Tianjin $PM_{2.5}$ are depicted in Fig. 13. $\delta^{15}N_{TN}$ in Tianjin $PM_{2.5}$ is slightly higher than that (−19.4 ‰ to 15.4 ‰) reported for the particles emitted from point sources of fossil fuel combustion and waste incineration burning (Fig. 13). They are also higher than those reported in the marine aerosols over the western North Pacific (4.9 ± 2.8 ‰), which were considered to be mainly derived from sea-to-air emissions (Miyazaki et al., 2011). However, $\delta^{15}N_{TN}$ in Tianjin $PM_{2.5}$ are comparable to the higher ends of the $\delta^{15}N_{TN}$ reported in atmospheric aerosols from Jeju Island, Korea (Fig. 13), which were attributed to vehicle emissions, coal burning and straw burning (Kundu et al., 2010), and to those reported in urban aerosols from Paris, France, where fossil fuel combustion was expected to be a major source (Widory, 2007). Furthermore, the lower ends of $\delta^{15}N_{TN}$ in Tianjin $PM_{2.5}$ are comparable to the lower ends of $\delta^{15}N_{TN}$ reported for the particles emitted from the controlled burning of C_3 plant debris (range: +2.0 ‰ to +19.5 ‰) (Fig. 13). The higher ends of $\delta^{15}N_{TN}$ in Tianjin $PM_{2.5}$ are comparable to the higher ends of $\delta^{15}N_{TN}$ from C_4 plant debris (+9.8 ‰ to +22.7 ‰) in a laboratory study and to those of atmospheric aerosols from Piracicaba and the Amazon basin, Brazil, where biomass burning is a dominant source (Cloern et al., 2002) (Fig. 13). This is consistent with the fact that wheat and corn are the main crops in Tianjin. Such comparisons again confirm that biomass burning is a major source of atmospheric aerosols, followed by fossil fuel combustion in the Tianjin region.

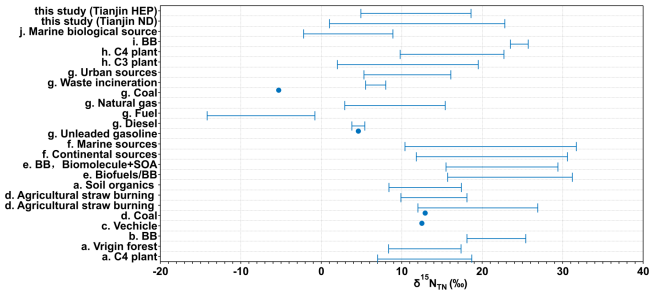

Figure 13. Range or mean $\delta^{15}N_{TN}$ in the particles emitted from point sources, source substances, and atmospheric aerosols from different sites around the world. **(a)** Martinelli et al. (2002); **(b)** Aggarwal et al. (2013); **(c)** Kunwar et al. (2016); **(d)** Kundu et al. (2010); **(e)** Pavuluri et al. (2010); **(f)** Bikkina et al. (2016); **(g)** Widory (2007); **(h)** Turekian et al. (1998); **(i)** Kundu et al. (2010); **(j)** Miyazaki et al. (2011).

4 Summary and conclusions

Fine aerosol ($PM_{2.5}$) samples were collected with a frequency of 3 consecutive days for each sample over a 1-year period from July 2018 to July 2019 at urban (ND) and suburban (HEP) sites in the Tianjin atmosphere, North China. The $PM_{2.5}$ was studied for carbonaceous (OC, EC, WSOC, WIOC, SOC and TC), nitrogenous (WSTN, IN and WSON), and inorganic ionic (Cl^-, NO_3^-, SO_4^{2-}, Na^+, K^+, NH_4^+, Ca^{2+} and Mg^{2+}) components as well as stable carbon and nitrogen isotope ratios of total carbon ($\delta^{13}C_{TC}$) and nitrogen ($\delta^{15}N_{TN}$). The characteristics of $PM_{2.5}$ and its components showed a clear seasonal pattern, with higher concentrations in winter and lower concentrations mostly in summer. The mass ratios of OC/EC, WSOC/OC and SOC/OC suggested that Tianjin aerosols were derived from coal combustion, biomass burning and photochemical reactions of VOCs and also implied that the Tianjin aerosols were more aged during long-range atmospheric transport in summer. The seasonal variation in ion concentrations highlighted that coal combustion was the main source of aerosol and that automobile exhaust also played an important role in controlling the Tianjin aerosol loading. In addition, the concentration of SO_4^{2-} at HEP peaked in summer and was at its minimum in autumn, and the overall levels were higher at HEP than those at ND Tianjin, which suggested that the contribution of the marine air masses originated from the oceanic region in summer and sea breeze throughout the year, and industrial emissions, particularly from the petrochemical industry located at the seashore, were larger at HEP than at ND. The values of $\delta^{13}C_{TC}$ and $\delta^{15}N_{TN}$ also showed that biomass and coal combustion were the major sources of aerosols in autumn and winter, and dust, biological emissions and the oceanic emissions were major in spring and summer in Tianjin. Moreover, this study has also provided comprehensive baseline data on carbonaceous and inorganic aerosols as well as their isotope ratios over a 1-year period in the Tianjin region, North China.

Data availability. The data used in this study can be found online at https://doi.org/10.5281/zenodo.5140861 (Dong et al., 2021).

Author contributions. ZD and CMP conceptualized this study. ZD, YW and PL conducted the sampling. ZD conducted the chem-

ical analyses, interpreted the data and wrote the manuscript. CMP supervised the research and acquired the funding for this study. ZX administrated the project. CMP, ZX, PF and CQL contributed in discussing the results and review and editing the manuscript.

Competing interests. The contact author has declared that none of the authors has any competing interests.

Disclaimer. Publisher's note: Copernicus Publications remains neutral with regard to jurisdictional claims in published maps and institutional affiliations.

Financial support. This research has been supported by the National Key Research and Development Program of China (grant no. 2017YFC0212700) and the National Natural Science Foundation of China (grant no. 41775120).

Review statement. This paper was edited by Zhibin Wang and reviewed by two anonymous referees.

References

Aggarwal, S. G. and Kawamura, K.: Carbonaceous and inorganic composition in long-range transported aerosols over northern Japan: Implication for aging of water-soluble organic fraction, Atmos. Environ., 43, 2532–2540, https://doi.org/10.1016/j.atmosenv.2009.02.032, 2009.

Aggarwal, S. G., Kawamura, K., Umarji, G. S., Tachibana, E., Patil, R. S., and Gupta, P. K.: Organic and inorganic markers and stable C-, N-isotopic compositions of tropical coastal aerosols from megacity Mumbai: sources of organic aerosols and atmospheric processing, Atmos. Chem. Phys., 13, 4667–4680, https://doi.org/10.5194/acp-13-4667-2013, 2013.

Andreae, M. O., Schmid, O., Yang, H., Chand, D., Zhen Yu, J., Zeng, L.-M., and Zhang, Y.-H.: Optical properties and chemical composition of the atmospheric aerosol in urban Guangzhou, China, Atmos. Environ., 42, 6335–6350, https://doi.org/10.1016/j.atmosenv.2008.01.030, 2008.

Ballentine, D. C., Macko, S. A., and Turekian, V. C.: Variability of stable carbon isotopic compositions in individual fatty acids from combustion of C_4 and C_3 plants: implications for biomass burning, Chem. Geol., 152, 151–161, https://doi.org/10.1016/S0009-2541(98)00103-X, 1998.

Behera, S. N., Betha, R., and Balasubramanian, R.: Insights into Chemical Coupling among Acidic Gases, Ammonia and Secondary Inorganic Aerosols, Aerosol Air Qual. Res., 13, 1282–1296, https://doi.org/10.4209/aaqr.2012.11.0328, 2013.

Bei, N., Zhao, L., Wu, J., Li, X., Feng, T., and Li, G.: Impacts of sea-land and mountain-valley circulations on the air pollution in Beijing-Tianjin-Hebei (BTH): A case study, Environ. Pollut., 234, 429–438, 2018.

Bencs, L., Ravindra, K., de Hoog, J., Spolnik, Z., Bleux, N., Berghmans, P., Deutsch, F., Roekens, E., and Van Grieken, R.: Appraisal of measurement methods, chemical composition and sources of fine atmospheric particles over six different areas of Northern Belgium, Environ. Pollut., 158, 3421–3430, https://doi.org/10.1016/j.envpol.2010.07.012, 2010.

Bikkina, S., Kawamura, K., and Sarin, M.: Stable carbon and nitrogen isotopic composition of fine mode aerosols ($PM_{2.5}$) over the Bay of Bengal: impact of continental sources, Tellus B, 68, 31518, https://doi.org/10.3402/tellusb.v68.31518, 2016.

Bikkina, S., Andersson, A., Ram, K., Sarin, M. M., Sheesley, R. J., Kirillova, E. N., Rengarajan, R., Sudheer, A. K., and Gustafsson, O.: Carbon isotope-constrained seasonality of carbonaceous aerosol sources from an urban location (Kanpur) in the Indo-Gangetic Plain, J. Geophys. Res.-Atmos., 122, 4903–4923, https://doi.org/10.1002/2016jd025634, 2017a.

Bikkina, S., Kawamura, K., and Sarin, M.: Secondary organic aerosol formation over coastal ocean: Inferences from atmospheric water-soluble low molecular weight organic compounds, Environ. Sci. Technol., 51, 4347–4357, https://doi.org/10.1021/acs.est.6b05986, 2017b.

Blanchard, C. L. and Hidy, G. M.: Effects of changes in sulfate, ammonia, and nitric acid on particulate nitrate concentrations in the southeastern United States, J. Air Waste Manage., 53, 283–290, 2003.

Brown, S. S. and Stutz, J.: Nighttime radical observations and chemistry, Chem. Soc. Rev., 41, 6405–6447, 2012.

Cachier, H., Buat-Ménard, M. P., Fontugne, M., and Chesselet, R.: Long–range transport of continentally–derived particulate carbon in the marine atmosphere: Evidence from stable carbon isotope studies, Tellus B, 38, 161–177, https://doi.org/10.3402/tellusb.v38i3-4.15125, 1986.

Cao, F., Zhang, S. C., Kawamura, K., and Zhang, Y. L.: Inorganic markers, carbonaceous components and stable carbon isotope from biomass burning aerosols in Northeast China, Sci. Total Environ., 572, 1244–1251, https://doi.org/10.1016/j.scitotenv.2015.09.099, 2016.

Cao, J. J., Lee, S. C., Chow, J. C., Watson, J. G., Ho, K. F., Zhang, R. J., Jin, Z. D., Shen, Z. X., Chen, G. C., Kang, Y. M., Zou, S. C., Zhang, L. Z., Qi, S. H., Dai, M. H., Cheng, Y., and Hu, K.: Spatial and seasonal distributions of carbonaceous aerosols over China, J. Geophys. Res., 112, D22S11, https://doi.org/10.1029/2006jd008205, 2007.

Cao, J. J., Chow, J. C., Tao, J., Lee, S. C., Watson, J. G., Ho, K. F., Wang, G. H., Zhu, C. S., and Han, Y. M.: Stable carbon isotopes in aerosols from Chinese cities: Influence of fossil fuels, Atmos. Environ., 45, 1359–1363, https://doi.org/10.1016/j.atmosenv.2010.10.056, 2011.

Cape, J. N., Cornell, S. E., Jickells, T. D., and Nemitz, E.: Organic nitrogen in the atmosphere – Where does it come from? A review of sources and methods, Atmos. Res., 102, 30–48, https://doi.org/10.1016/j.atmosres.2011.07.009, 2011.

Chen, Q.-X., Huang, C.-L., Xiao, T., Yuan, Y., Mao, Q.-J., and Tan, H.-P.: Characterization of atmospheric aerosols and source apportionment analyses in urban Harbin, northeast China, Infrared Phys. Techn., 103, 103109, https://doi.org/10.1016/j.infrared.2019.103109, 2019.

Chen, Y., Zheng, M., Edgerton, E. S., Ke, L., Sheng, G., and Fu, J.: $PM_{2.5}$ source apportionment in the southeastern U.S.: Spatial and seasonal variations during 2001–2005, J. Geophys. Res.-Atmos., 117, D08304, https://doi.org/10.1029/2011JD016572, 2012.

Chesselet, R., Fontugne, M., Buat-Ménard, P., Ezat, U., and Lambert, C. E.: The origin of particulate organic carbon in the marine atmosphere as indicated by its stable carbon isotopic composition, Geophys. Res. Lett., 8, 345–348, https://doi.org/10.1029/GL008i004p00345, 1981.

Chow, J. C., Bachmann, J. D., Wierman, S. S. G., Mathai, C. V., Malm, W. C., White, W. H., Mueller, P. K., Kumar, N., and Watson, J. G.: Visibility: Science and Regulation, J. Air Waste Manage., 52, 973–999, https://doi.org/10.1080/10473289.2002.10470844, 2002.

Chow, J. C., Watson, J. G., Mauderly, J. L., Costa, D. L., Wyzga, R. E., Vedal, S., Hidy, G. M., Altshuler, S. L., Marrack, D., Heuss, J. M., Wolff, G. T., Arden Pope III, C., and Dockery, D. W.: Health Effects of Fine Particulate Air Pollution: Lines that Connect, J. Air Waste Manage., 56, 1368–1380, https://doi.org/10.1080/10473289.2006.10464545, 2006.

Chow, J. C., Watson, J. G., Chen, L. W. A., Chang, M. C. O., Robinson, N. F., Trimble, D., and Kohl, S.: The IMPROVE_A Temperature Protocol for Thermal/Optical Carbon Analysis: Maintaining Consistency with a Long-Term Database, J. Air Waste Manage., 57, 1014–1023, https://doi.org/10.3155/1047-3289.57.9.1014, 2007.

Cloern, J. E., Canuel, E. A., and Harris, D.: Stable carbon and nitrogen isotope composition of aquatic and terrestrial plants of the San Francisco Bay estuarine system, Limnol. Oceanogr., 47, 713–729, https://doi.org/10.4319/lo.2002.47.3.0713, 2002.

Cui, H., Mao, P., Zhao, Y., Nielsen, C. P., and Zhang, J.: Patterns in atmospheric carbonaceous aerosols in China: emission estimates and observed concentrations, Atmos. Chem. Phys., 15, 8657–8678, https://doi.org/10.5194/acp-15-8657-2015, 2015.

Dan, M., Zhuang, G., Li, X., Tao, H., and Zhuang, Y.: The characteristics of carbonaceous species and their sources in $PM_{2.5}$ in Beijing, Atmos. Environ., 38, 3443–3452, https://doi.org/10.1016/j.atmosenv.2004.02.052, 2004.

Dentener, F., Drevet, J., Lamarque, J. F., Bey, I., Eickhout, B., Fiore, A. M., Hauglustaine, D., Horowitz, L. W., Krol, M., Kulshrestha, U. C., Lawrence, M., Galy-Lacaux, C., Rast, S., Shindell, D., Stevenson, D., Van Noije, T., Atherton, C., Bell, N., Bergman, D., Butler, T., Cofala, J., Collins, B., Doherty, R., Ellingsen, K., Galloway, J., Gauss, M., Montanaro, V., Müller, J. F., Pitari, G., Rodriguez, J., Sanderson, M., Solmon, F., Strahan, S., Schultz, M., Sudo, K., Szopa, S., and Wild, O.: Nitrogen and sulfur deposition on regional and global scales: A multimodel evaluation, Global Biogeochem. Cy., 20, GB4003, https://doi.org/10.1029/2005GB002672, 2006.

Dong, Z., Pavuluri, C. M., Xu, Z., Wang, Y., Li, P., Fu, P., and Liu, C.-Q.: Year-round observations of bulk components and ^{13}C and ^{15}N isotope ratios of fine aerosols at Tianjin, North China, Zenodo [data set], https://doi.org/10.5281/zenodo.5140861, 2021.

Draper, D. C., Myllys, N., Hyttinen, N., Møller, K. H., Kjaergaard, H. G., Fry, J. L., Smith, J. N., and Kurtén, T.: Formation of Highly Oxidized Molecules from NO_3 Radical Initiated Oxidation of Δ-3-Carene: A Mechanistic Study, ACS Earth Space Chem., 3, 1460–1470, 2019.

Duan, F., He, K., Ma, Y., Jia, Y., Yang, F., Lei, Y., Tanaka, S., and Okuta, T.: Characteristics of carbonaceous aerosols in Beijing, China, Chemosphere, 60, 355–364, https://doi.org/10.1016/j.chemosphere.2004.12.035, 2005.

Duarte, R. M. B. O., Piñeiro-Iglesias, M., López-Mahía, P., Muniategui-Lorenzo, S., Moreda-Piñeiro, J., Silva, A. M. S., and Duarte, A. C.: Comparative study of atmospheric water-soluble organic aerosols composition in contrasting suburban environments in the Iberian Peninsula Coast, Sci. Total Environ., 648, 430–441, https://doi.org/10.1016/j.scitotenv.2018.08.171, 2019.

Fajardie, F., Tempère, J.-F., Manoli, J.-M., Touret, O., Blanchard, G., and Djéga-Mariadassou, G.: Activity of Rh^{x+} Species in CO Oxidation and NO Reduction in a $CO/NO/O_2$ Stoichiometric Mixture over a Rh/CeO_2-ZrO_2 Catalyst, J. Catal., 179, 469–476, https://doi.org/10.1006/jcat.1998.2222, 1998.

Feng, J., Hu, M., Chan, C. K., Lau, P. S., Fang, M., He, L., and Tang, X.: A comparative study of the organic matter in $PM_{2.5}$ from three Chinese megacities in three different climatic zones, Atmos. Environ., 40, 3983–3994, https://doi.org/10.1016/j.atmosenv.2006.02.017, 2006.

Feng, Y., Chen, Y., Guo, H., Zhi, G., Xiong, S., Li, J., Sheng, G., and Fu, J.: Characteristics of organic and elemental carbon in $PM_{2.5}$ samples in Shanghai, China, Atmos. Res., 92, 434–442, https://doi.org/10.1016/j.atmosres.2009.01.003, 2009.

Freyer, H. D.: Seasonal trends of NH_4^+ and NO_3^- nitrogen isotope composition in rain collected at Jülich, Germany, Tellus, 30, 83–92, https://doi.org/10.3402/tellusa.v30i1.10319, 1978.

Fu, P. Q., Kawamura, K., Chen, J., Li, J., Sun, Y. L., Liu, Y., Tachibana, E., Aggarwal, S. G., Okuzawa, K., Tanimoto, H., Kanaya, Y., and Wang, Z. F.: Diurnal variations of organic molecular tracers and stable carbon isotopic composition in atmospheric aerosols over Mt. Tai in the North China Plain: an influence of biomass burning, Atmos. Chem. Phys., 12, 8359–8375, https://doi.org/10.5194/acp-12-8359-2012, 2012.

Galloway, J. N., Townsend, A. R., Erisman, J. W., Bekunda, M., Cai, Z., Freney, J. R., Martinelli, L. A., Seitzinger, S. P., and Sutton, M. A.: Transformation of the nitrogen cycle: recent trends, questions, and potential solutions, Science, 320, 889–892, https://doi.org/10.1126/science.1136674, 2008.

Garbaras, A., Masalaite, A., Garbariene, I., Ceburnis, D., Krugly, E., Remeikis, V., Puida, E., Kvietkus, K., and Martuzevicius, D.: Stable carbon fractionation in size-segregated aerosol particles produced by controlled biomass burning, J. Aerosol Sci., 79, 86–96, https://doi.org/10.1016/j.jaerosci.2014.10.005, 2015.

Gu, B., Chang, J., Min, Y., Ge, Y., Zhu, Q., Galloway, J. N., and Peng, C.: The role of industrial nitrogen in the global nitrogen biogeochemical cycle, Sci. Rep., 3, 2579, https://doi.org/10.1038/srep02579, 2013.

Gu, B., Ju, X., Chang, J., Ge, Y., and Vitousek, P. M.: Integrated reactive nitrogen budgets and future trends in China, P. Natl. Acad. Sci. USA, 112, 8792–8797, https://doi.org/10.1073/pnas.1510211112, 2015.

Gu, J., Bai, Z., Liu, A., Wu, L., Xie, Y., Li, W., Dong, H., and Zhang, X.: Characterization of atmospheric organic carbon and element carbon of $PM_{2.5}$ and PM_{10} at Tianjin, China, Aerosol Air Qual. Res., 10, 167–176, https://doi.org/10.4209/aaqr.2009.12.0080, 2010.

Hasheminassab, S., Daher, N., Shafer, M. M., Schauer, J. J., Delfino, R. J., and Sioutas, C.: Chemical characterization and source apportionment of indoor and outdoor fine particulate matter ($PM_{2.5}$) in retirement communities of the Los Angeles Basin, Sci. Total Environ., 490, 528–537, https://doi.org/10.1016/j.scitotenv.2014.05.044, 2014.

He, K., Yang, F., Ma, Y., Zhang, Q., Yao, X., Chan, C. K., Cadle, S., Chan, T., and Mulawa, P.: The characteristics of $PM_{2.5}$ in Beijing, China, Atmos. Environ., 35, 4959–4970, https://doi.org/10.1016/S1352-2310(01)00301-6, 2001.

Hoefs, J.: Stable Isotope Geochemistry, Springer, New York, ISBN 3-540-61126-6, 1997.

Huang, H., Ho, K. F., Lee, S. C., Tsang, P. K., Ho, S. S. H., Zou, C. W., Zou, S. C., Cao, J. J., and Xu, H. M.: Characteristics of carbonaceous aerosol in $PM_{2.5}$: Pearl Delta River Region, China, Atmos. Res., 104–105, 227–236, https://doi.org/10.1016/j.atmosres.2011.10.016, 2012.

Huang, R. J., Zhang, Y., Bozzetti, C., Ho, K. F., Cao, J. J., Han, Y., Daellenbach, K. R., Slowik, J. G., Platt, S. M., Canonaco, F., Zotter, P., Wolf, R., Pieber, S. M., Bruns, E. A., Crippa, M., Ciarelli, G., Piazzalunga, A., Schwikowski, M., Abbaszade, G., Schnelle-Kreis, J., Zimmermann, R., An, Z., Szidat, S., Baltensperger, U., El Haddad, I., and Prevot, A. S.: High secondary aerosol contribution to particulate pollution during haze events in China, Nature, 514, 218–222, https://doi.org/10.1038/nature13774, 2014.

Huang, X.-F., Xue, L., Tian, X.-D., Shao, W.-W., Sun, T.-L., Gong, Z.-H., Ju, W.-W., Jiang, B., Hu, M., and He, L.-Y.: Highly time-resolved carbonaceous aerosol characterization in Yangtze River Delta of China: Composition, mixing state and secondary formation, Atmos. Environ., 64, 200–207, https://doi.org/10.1016/j.atmosenv.2012.09.059, 2013.

Huang, Y., Liu, Y., Zhang, L., Peng, C., and Yang, F.: Characteristics of carbonaceous aerosol in $PM_{2.5}$ at Wanzhou in the Southwest of China, Atmosphere, 9, 37, https://doi.org/10.3390/atmos9020037, 2018.

Ji, D., Li, L., Wang, Y., Zhang, J., Cheng, M., Sun, Y., Liu, Z., Wang, L., Tang, G., Hu, B., Chao, N., Wen, T., and Miao, H.: The heaviest particulate air-pollution episodes occurred in northern China in January, 2013: Insights gained from observation, Atmos. Environ., 92, 546–556, https://doi.org/10.1016/j.atmosenv.2014.04.048, 2014.

Jickells, T. D., Kelly, S. D., Baker, A. R., Biswas, K., Dennis, P. F., Spokes, L. J., Witt, M., and Yeatman, S. G.: Isotopic evidence for a marine ammonia source, Geophys. Res. Lett., 30, 1374, https://doi.org/10.1029/2002gl016728, 2003.

Jimenez, J. L., Canagaratna, M. R., Donahue, N. M., Prevot, A. S., Zhang, Q., Kroll, J. H., DeCarlo, P. F., Allan, J. D., Coe, H., Ng, N. L., Aiken, A. C., Docherty, K. S., Ulbrich, I. M., Grieshop, A. P., Robinson, A. L., Duplissy, J., Smith, J. D., Wilson, K. R., Lanz, V. A., Hueglin, C., Sun, Y. L., Tian, J., Laaksonen, A., Raatikainen, T., Rautiainen, J., Vaattovaara, P., Ehn, M., Kulmala, M., Tomlinson, J. M., Collins, D. R., Cubison, M. J., Dunlea, E. J., Huffman, J. A., Onasch, T. B., Alfarra, M. R., Williams, P. I., Bower, K., Kondo, Y., Schneider, J., Drewnick, F., Borrmann, S., Weimer, S., Demerjian, K., Salcedo, D., Cottrell, L., Griffin, R., Takami, A., Miyoshi, T., Hatakeyama, S., Shimono, A., Sun, J. Y., Zhang, Y. M., Dzepina, K., Kimmel, J. R., Sueper, D., Jayne, J. T., Herndon, S. C., Trimborn, A. M., Williams, L. R., Wood, E. C., Middlebrook, A. M., Kolb, C. E., Baltensperger, U., and Worsnop, D. R.: Evolution of organic aerosols in the atmosphere, Science, 326, 1525–1529, https://doi.org/10.1126/science.1180353, 2009.

Kawamura, K., Kobayashi, M., Tsubonuma, N., Mochida, M., Watanabe, T., and Lee, M.: Organic and inorganic compositions of marine aerosols from East Asia: Seasonal variations of water-soluble dicarboxylic acids, major ions, total carbon and nitrogen, and stable C and N isotopic composition, in: Geochemical Investigation in Earth and Space Science: A Tribute to Isaac R. Kaplan, edited by: Hill, R. J., Leventhal, J., Aizenshtat, Z., Baedecker, M. J., Claypool, G., Eganhouse, R., Goldhaber, M., and Peters, K., The Geochemical Society, Publication No. 9, 243–265, 2004.

Kiss, G., Varga, B., Galambos, I., and Ganszky, I.: Characterization of water-soluble organic matter isolated from atmospheric fine aerosol, J. Geophys. Res.-Atmos., 107, ICC 1-1–ICC 1-8, https://doi.org/10.1029/2001jd000603, 2002.

Kong, S., Han, B., Bai, Z., Chen, L., Shi, J., and Xu, Z.: Receptor modeling of $PM_{2.5}$, PM_{10} and TSP in different seasons and long-range transport analysis at a coastal site of Tianjin, China, Sci. Total Environ., 408, 4681–4694, https://doi.org/10.1016/j.scitotenv.2010.06.005, 2010.

Kundu, S., Kawamura, K., and Lee, M.: Seasonal variation of the concentrations of nitrogenous species and their nitrogen isotopic ratios in aerosols at Gosan, Jeju Island: Implications for atmospheric processing and source changes of aerosols, J. Geophys. Res., 115, D20305, https://doi.org/10.1029/2009jd013323, 2010.

Kunwar, B., Kawamura, K., and Zhu, C.: Stable carbon and nitrogen isotopic compositions of ambient aerosols collected from Okinawa Island in the western North Pacific Rim, an outflow region of Asian dusts and pollutants, Atmos. Environ., 131, 243–253, https://doi.org/10.1016/j.atmosenv.2016.01.035, 2016.

Laden, F., Neas, L. M., Dockery, D. W., and Schwartz, J.: Association of fine particulate matter from different sources with daily mortality in six U.S. cities, Environ. Health Persp., 108, 941–947, https://doi.org/10.1289/ehp.00108941, 2000.

Lai, S., Zhao, Y., Ding, A., Zhang, Y., Song, T., Zheng, J., Ho, K. F., Lee, S.-C., and Zhong, L.: Characterization of $PM_{2.5}$ and the major chemical components during a 1-year campaign in rural Guangzhou, Southern China, Atmos. Res., 167, 208–215, https://doi.org/10.1016/j.atmosres.2015.08.007, 2016.

Larson, S. M. and Cass, G. R.: Characteristics of summer midday low-visibility events in the Los Angeles area, Environ. Sci. Technol., 23, 281–289, https://doi.org/10.1021/es00180a003, 1989.

Li, H., Wang, Q. g., Yang, M., Li, F., Wang, J., Sun, Y., Wang, C., Wu, H., and Qian, X.: Chemical characterization and source apportionment of $PM_{2.5}$ aerosols in a megacity of Southeast China, Atmos. Res., 181, 288–299, https://doi.org/10.1016/j.atmosres.2016.07.005, 2016.

Li, M., Hu, M., Du, B., Guo, Q., Tan, T., Zheng, J., Huang, X., He, L., Wu, Z., and Guo, S.: Temporal and spatial distribution of $PM_{2.5}$ chemical composition in a coastal city of Southeast China, Sci.Total Environ., 605–606, 337–346, https://doi.org/10.1016/j.scitotenv.2017.03.260, 2017.

Li, P., Pavuluri, C. M., Dong, Z., Xu, Z., Wang, Y., Fu, P., and Liu, C. Q.: Characteristics, Seasonality, and Secondary Formation Processes of Diacids and Related Compounds in Fine Aerosols During Warm and Cold Periods: Year-Round Observations at Tianjin, North China, J. Geophys. Res.-Atmos., 126, e2021JD035435, https://doi.org/10.1029/2021JD035435, 2021.

Li, P., Pavuluri, C. M., Dong, Z., Xu, Z., Fu, P., and Liu, C.-Q.: Year-round observations of stable carbon isotopic composition of carboxylic acids, oxoacids and α-Dicarbonyls in fine aerosols at Tianjin, North China: Implica-

tions for origins and aging, Sci. Total Environ., 834, 155385, https://doi.org/10.1016/j.scitotenv.2022.155385, 2022.

Li, P.-H., Han, B., Huo, J., Lu, B., Ding, X., Chen, L., Kong, S.-F., Bai, Z.-P., and Wang, B.: Characterization, Meteorological Influences and Source Identification of Carbonaceous Aerosols during the Autumn-winter Period in Tianjin, China, Aerosol Air Qual. Res., 12, 283–294, https://doi.org/10.4209/aaqr.2011.09.0140, 2012.

Li, W., Bai, Z., Liu, A., Chen, J., and Chen, L.: Characteristics of Major $PM_{2.5}$ Components during Winter in Tianjin, China, Aerosol Air Qual. Res., 9, 105–119, https://doi.org/10.4209/aaqr.2008.11.0054, 2009.

Li, X., Zhang, Q., Zhang, Y., Zhang, L., Wang, Y., Zhang, Q., Li, M., Zheng, Y., Geng, G., Wallington, T. J., Han, W., Shen, W., and He, K.: Attribution of $PM_{2.5}$ exposure in Beijing–Tianjin–Hebei region to emissions: implication to control strategies, Sci. Bull., 62, 957–964, https://doi.org/10.1016/j.scib.2017.06.005, 2017.

Lim, S. S., Vos, T., Flaxman, A. D., Danaei, G., Shibuya, K., Adair-Rohani, H., AlMazroa, M. A., Amann, M., Anderson, H. R., Andrews, K. G., Aryee, M., Atkinson, C., Bacchus, L. J., Bahalim, A. N., Balakrishnan, K., Balmes, J., Barker-Collo, S., Baxter, A., Bell, M. L., Blore, J. D., Blyth, F., Bonner, C., Borges, G., Bourne, R., Boussinesq, M., Brauer, M., Brooks, P., Bruce, N. G., Brunekreef, B., Bryan-Hancock, C., Bucello, C., Buchbinder, R., Bull, F., Burnett, R. T., Byers, T. E., Calabria, B., Carapetis, J., Carnahan, E., Chafe, Z., Charlson, F., Chen, H., Chen, J. S., Cheng, A. T.-A., Child, J. C., Cohen, A., Colson, K. E., Cowie, B. C., Darby, S., Darling, S., Davis, A., Degenhardt, L., Dentener, F., Des Jarlais, D. C., Devries, K., Dherani, M., Ding, E. L., Dorsey, E. R., Driscoll, T., Edmond, K., Ali, S. E., Engell, R. E., Erwin, P. J., Fahimi, S., Falder, G., Farzadfar, F., Ferrari, A., Finucane, M. M., Flaxman, S., Fowkes, F. G. R., Freedman, G., Freeman, M. K., Gakidou, E., Ghosh, S., Giovannucci, E., Gmel, G., Graham, K., Grainger, R., Grant, B., Gunnell, D., Gutierrez, H. R., Hall, W., Hoek, H. W., Hogan, A., Hosgood III, H. D., Hoy, D., Hu, H., Hubbell, B. J., Hutchings, S. J., Ibeanusi, S. E., Jacklyn, G. L., Jasrasaria, R., Jonas, J. B., Kan, H., Kanis, J. A., Kassebaum, N., Kawakami, N., Khang, Y.-H., Khatibzadeh, S., Khoo, J.-P., Kok, C., Laden, F., Lalloo, R., Lan, Q., Lathlean, T., Leasher, J. L., Leigh, J., Li, Y., Lin, J. K., Lipshultz, S. E., London, S., Lozano, R., Lu, Y., Mak, J., Malekzadeh, R., Mallinger, L., Marcenes, W., March, L., Marks, R., Martin, R., McGale, P., McGrath, J., Mehta, S., Memish, Z. A., Mensah, G. A., Merriman, T. R., Micha, R., Michaud, C., Mishra, V., Hanafiah, K. M., Mokdad, A. A., Morawska, L., Mozaffarian, D., Murphy, T., Naghavi, M., Neal, B., Nelson, P. K., Nolla, J. M., Norman, R., Olives, C., Omer, S. B., Orchard, J., Osborne, R., Ostro, B., Page, A., Pandey, K. D., Parry, C. D. H., Passmore, E., Patra, J., Pearce, N., Pelizzari, P. M., Petzold, M., Phillips, M. R., Pope, D., Pope III, C. A., Powles, J., Rao, M., Razavi, H., Rehfuess, E. A., Rehm, J. T., Ritz, B., Rivara, F. P., Roberts, T., Robinson, C., Rodriguez-Portales, J. A., Romieu, I., Room, R., Rosenfeld, L. C., Roy, A., Rushton, L., Salomon, J. A., Sampson, U., Sanchez-Riera, L., Sanman, E., Sapkota, A., Seedat, S., Shi, P., Shield, K., Shivakoti, R., Singh, G. M., Sleet, D. A., Smith, E., Smith, K. R., Stapelberg, N. J. C., Steenland, K., Stöckl, H., Stovner, L. J., Straif, K., Straney, L., Thurston, G. D., Tran, J. H., Van Dingenen, R., van Donkelaar, A., Veerman, J. L., Vijayakumar, L., Weintraub, R., Weissman, M. M., White, R. A., Whiteford, H., Wiersma, S. T., Wilkinson, J. D., Williams, H. C., Williams, W., Wilson, N., Woolf, A. D., Yip, P., Zielinski, J. M., Lopez, A. D., Murray, C. J. L., and Ezzati, M.: A comparative risk assessment of burden of disease and injury attributable to 67 risk factors and risk factor clusters in 21 regions, 1990–2010: a systematic analysis for the Global Burden of Disease Study 2010, Lancet, 380, 2224–2260, https://doi.org/10.1016/S0140-6736(12)61766-8, 2012.

Liu, Z., Liu, Q., Lin, H. C., Schwartz, C. S., Lee, Y. H., and Wang, T.: Three-dimensional variational assimilation of MODIS aerosol optical depth: Implementation and application to a dust storm over East Asia, J. Geophys. Res.-Atmos., 116, D23206, https://doi.org/10.1029/2011JD016159, 2011.

Luo, Y., Zhou, X., Zhang, J., Xiao, Y., Wang, Z., Zhou, Y., and Wang, W.: $PM_{2.5}$ pollution in a petrochemical industry city of northern China: Seasonal variation and source apportionment, Atmos. Res., 212, 285–295, https://doi.org/10.1016/j.atmosres.2018.05.029, 2018.

Lyu, X.-P., Wang, Z.-W., Cheng, H.-R., Zhang, F., Zhang, G., Wang, X.-M., Ling, Z.-H., and Wang, N.: Chemical characteristics of submicron particulates ($PM_{1.0}$) in Wuhan, Central China, Atmos. Res., 161–162, 169–178, https://doi.org/10.1016/j.atmosres.2015.04.009, 2015.

Martinelli, L. A., Camargo, P. B., Lara, L. B. L. S., Victoria, R. L., and Artaxo, P.: Stable carbon and nitrogen isotopic composition of bulk aerosol particles in a C_4 plant landscape of southeast Brazil, Atmos. Environ., 36, 2427–2432, https://doi.org/10.1016/S1352-2310(01)00454-X, 2002.

Matsumoto, K., Takusagawa, F., Suzuki, H., and Horiuchi, K.: Water-soluble organic nitrogen in the aerosols and rainwater at an urban site in Japan: Implications for the nitrogen composition in the atmospheric deposition, Atmos. Environ., 191, 267–272, https://doi.org/10.1016/j.atmosenv.2018.07.056, 2018.

McNeill, V. F., Woo, J. L., Kim, D. D., Schwier, A. N., Wannell, N. J., Sumner, A. J., and Barakat, J. M.: Aqueous-phase secondary organic aerosol and organosulfate formation in atmospheric aerosols: A modeling study, Environ. Sci. Technol., 46, 8075–8081, https://doi.org/10.1021/es3002986, 2012.

Menon, S., Hansen, J., Nazarenko, L., and Luo, Y.: Climate effects of black carbon aerosols in China and India, Science, 297, 2250–2253, https://doi.org/10.1126/science.1075159, 2002.

Ming, L., Jin, L., Li, J., Fu, P., Yang, W., Liu, D., Zhang, G., Wang, Z., and Li, X.: $PM_{2.5}$ in the Yangtze River Delta, China: Chemical compositions, seasonal variations, and regional pollution events, Environ. Pollut., 223, 200–212, https://doi.org/10.1016/j.envpol.2017.01.013, 2017.

Miyazaki, Y., Kawamura, K., Jung, J., Furutani, H., and Uematsu, M.: Latitudinal distributions of organic nitrogen and organic carbon in marine aerosols over the western North Pacific, Atmos. Chem. Phys., 11, 3037–3049, https://doi.org/10.5194/acp-11-3037-2011, 2011.

Mkoma, S. L., Kawamura, K., Tachibana, E., and Fu, P.: Stable carbon and nitrogen isotopic compositions of tropical atmospheric aerosols: sources and contribution from burning of C_3 and C_4 plants to organic aerosols, Tellus B, 66, 20176, 10.3402/tellusb.v66.20176, 2014.

Moore, H.: Isotopic measurement of atmospheric nitrogen compounds, Tellus, 26, 169–174, https://doi.org/10.3402/tellusa.v26i1-2.9767, 1974.

Morin, S., Savarino, J., Frey, M. M., Domine, F., Jacobi, H.-W., Kaleschke, L., and Martins, J. M. F.: Comprehensive isotopic composition of atmospheric nitrate in the Atlantic Ocean boundary layer from 65° S to 79° N, J. Geophys. Res.-Atmos., 114, D05303, https://doi.org/10.1029/2008jd010696, 2009.

Ng, N. L., Brown, S. S., Archibald, A. T., Atlas, E., Cohen, R. C., Crowley, J. N., Day, D. A., Donahue, N. M., Fry, J. L., Fuchs, H., Griffin, R. J., Guzman, M. I., Herrmann, H., Hodzic, A., Iinuma, Y., Jimenez, J. L., Kiendler-Scharr, A., Lee, B. H., Luecken, D. J., Mao, J., McLaren, R., Mutzel, A., Osthoff, H. D., Ouyang, B., Picquet-Varrault, B., Platt, U., Pye, H. O. T., Rudich, Y., Schwantes, R. H., Shiraiwa, M., Stutz, J., Thornton, J. A., Tilgner, A., Williams, B. J., and Zaveri, R. A.: Nitrate radicals and biogenic volatile organic compounds: oxidation, mechanisms, and organic aerosol, Atmos. Chem. Phys., 17, 2103–2162, https://doi.org/10.5194/acp-17-2103-2017, 2017.

Ottley, C. J. and Harrison, R. M.: The spatial distribution and particle size of some inorganic nitrogen, sulphur and chlorine species over the North Sea, Atmos. Environ. A-Gen., 26, 1689–1699, https://doi.org/10.1016/0960-1686(92)90067-U, 1992.

Padhy, P. and Varshney, C.: Emission of volatile organic compounds (VOC) from tropical plant species in India, Chemosphere, 59, 1643–1653, 2005.

Pavuluri, C. M. and Kawamura, K.: Enrichment of ^{13}C in diacids and related compounds during photochemical processing of aqueous aerosols: New proxy for organic aerosols aging, Sci. Rep.-UK, 6, 36467, https://doi.org/10.1038/srep36467, 2016.

Pavuluri, C. M. and Kawamura, K.: Seasonal changes in TC and WSOC and their ^{13}C isotope ratios in Northeast Asian aerosols: land surface–biosphere–atmosphere interactions, Acta Geochim., 36, 355–358, https://doi.org/10.1007/s11631-017-0157-3, 2017.

Pavuluri, C. M., Kawamura, K., Tachibana, E., and Swaminathan, T.: Elevated nitrogen isotope ratios of tropical Indian aerosols from Chennai: Implication for the origins of aerosol nitrogen in South and Southeast Asia, Atmos. Environ., 44, 3597–3604, https://doi.org/10.1016/j.atmosenv.2010.05.039, 2010.

Pavuluri, C. M., Kawamura, K., Aggarwal, S. G., and Swaminathan, T.: Characteristics, seasonality and sources of carbonaceous and ionic components in the tropical aerosols from Indian region, Atmos. Chem. Phys., 11, 8215–8230, https://doi.org/10.5194/acp-11-8215-2011, 2011.

Pavuluri, C. M., Kawamura, K., Uchida, M., Kondo, M., and Fu, P.: Enhanced modern carbon and biogenic organic tracers in Northeast Asian aerosols during spring/summer, J. Geophys. Res.-Atmos., 118, 2362–2371, https://doi.org/10.1002/jgrd.50244, 2013.

Pavuluri, C. M., Kawamura, K., and Fu, P. Q.: Atmospheric chemistry of nitrogenous aerosols in northeastern Asia: biological sources and secondary formation, Atmos. Chem. Phys., 15, 9883–9896, https://doi.org/10.5194/acp-15-9883-2015, 2015a.

Pavuluri, C. M., Kawamura, K., Mihalopoulos, N., and Fu, P.: Characteristics, seasonality and sources of inorganic ions and trace metals in North-east Asian aerosols, Environ. Chem., 12, 338–349, https://doi.org/10.1071/EN14186, 2015b.

Pavuluri, C. M., Kawamura, K., and Swaminathan, T.: Time-resolved distributions of bulk parameters, diacids, ketoacids and α-dicarbonyls and stable carbon and nitrogen isotope ratios of TC and TN in tropical Indian aerosols: Influence of land/sea breeze and secondary processes, Atmos. Res., 153, 188–199, https://doi.org/10.1016/j.atmosres.2014.08.011, 2015c.

Perri, M. J., Lim, Y. B., Seitzinger, S. P., and Turpin, B. J.: Organosulfates from glycolaldehyde in aqueous aerosols and clouds: Laboratory studies, Atmos. Environ., 44, 2658–2664, https://doi.org/10.1016/j.atmosenv.2010.03.031, 2010.

Pöschl, U.: Atmospheric Aerosols: Composition, Transformation, Climate and Health Effects, 37, 7520–7540, https://doi.org/10.1002/chin.200607299, 2006.

Ramanathan, V., Crutzen, P. J., Kiehl, J. T., and Rosenfeld, D.: Aerosols, climate, and the hydrological cycle, Science, 294, 2119–2124, https://doi.org/10.1126/science.1064034, 2001.

Robinson, A. L., Donahue, N. M., Shrivastava, M. K., Weitkamp, E. A., Sage, A. M., Grieshop, A. P., Lane, T. E., Pierce, J. R., and Pandis, S. N.: Rethinking organic aerosols: semivolatile emissions and photochemical aging, Science, 315, 1259–1262, https://doi.org/10.1126/science.1133061, 2007.

Rudolph, J.: Stable Carbon Isotope Ratio Measurements: A New Tool to Understand Atmospheric Processing of Volatile Organic Compounds, in: Global Atmospheric Change and its Impact on Regional Air Quality, edited by: Barnes, I., Springer Netherlands, Dordrecht, 37–42, 2002.

Russell, A. G., Mcrae, G. J., and Cass, G. R.: Mathematical modeling of the formation and transport of ammonium nitrate aerosol, Atmos. Environ., 17, 949–964, 1983.

Samet, J. M., Zeger, S. L., Dominici, F., Curriero, F., Coursac, I., Dockery, D. W., Schwartz, J., and Zanobetti, A.: The National Morbidity, Mortality, and Air Pollution Study. Part II: Morbidity and mortality from air pollution in the United States, Research report (Health Effects Institute), 94, 5–70, discussion 71–79, 2000.

Schaap, M., Spindler, G., Schulz, M., Acker, K., Maenhaut, W., Berner, A., Wieprecht, W., Streit, N., Müller, K., and Brüggemann, E.: Artefacts in the sampling of nitrate studied in the "INTERCOMP" campaigns of EUROTRAC-AEROSOL, Atmos. Environ., 38, 6487–6496, 2004.

Schwartz, J., Dockery, D. W., and Neas, L. M.: Is Daily Mortality Associated Specifically with Fine Particles?, J. Air Waste Manage., 46, 927–939, https://doi.org/10.1080/10473289.1996.10467528, 1996.

Sillanpää, M., Frey, A., Hillamo, R., Pennanen, A. S., and Salonen, R. O.: Organic, elemental and inorganic carbon in particulate matter of six urban environments in Europe, Atmos. Chem. Phys., 5, 2869–2879, https://doi.org/10.5194/acp-5-2869-2005, 2005.

Song, J., Zhao, Y., Zhang, Y., Fu, P., Zheng, L., Yuan, Q., Wang, S., Huang, X., Xu, W., Cao, Z., Gromov, S., and Lai, S.: Influence of biomass burning on atmospheric aerosols over the western South China Sea: Insights from ions, carbonaceous fractions and stable carbon isotope ratios, Environ. Pollut., 242, 1800–1809, https://doi.org/10.1016/j.envpol.2018.07.088, 2018.

Tao, J., Zhang, L., Ho, K., Zhang, R., Lin, Z., Zhang, Z., Lin, M., Cao, J., Liu, S., and Wang, G.: Impact of $PM_{2.5}$ chemical compositions on aerosol light scattering in Guangzhou – the largest megacity in South China, Atmos. Res., 135–136, 48–58, https://doi.org/10.1016/j.atmosres.2013.08.015, 2014.

Turekian, V. C., Macko, S., Ballentine, D., Swap, R. J., and Garstang, M.: Causes of bulk carbon and nitrogen isotopic fractionations in the products of vegetation burns: laboratory studies, Chem. Geol., 152, 181–192, https://doi.org/10.1016/S0009-2541(98)00105-3, 1998.

Turekian, V. C., Macko, S. A., and Keene, W. C.: Concentrations, isotopic compositions, and sources of size-resolved, particulate organic carbon and oxalate in near-surface marine air at Bermuda during spring, J. Geophys. Res.-Atmos., 108, 4157, https://doi.org/10.1029/2002jd002053, 2003.

Turpin, B. J. and Huntzicker, J. J.: Identification of secondary organic aerosol episodes and quantitation of primary and secondary organic aerosol concentrations during SCAQS, Atmos. Environ., 29, 3527–3544, https://doi.org/10.1016/1352-2310(94)00276-Q, 1995.

Turpin, B. J., Saxena, P., and Andrews, E.: Measuring and simulating particulate organics in the atmosphere: problems and prospects, Atmos. Environ., 34, 2983–3013, https://doi.org/10.1016/S1352-2310(99)00501-4, 2000.

Utsunomiya, A. and Wakamatsu, S.: Temperature and humidity dependence on aerosol composition in the northern Kyushu, Japan, Atmos. Environ., 30, 2379–2386, 1996.

Wan, X., Kang, S., Wang, Y., Xin, J., Liu, B., Guo, Y., Wen, T., Zhang, G., and Cong, Z.: Size distribution of carbonaceous aerosols at a high-altitude site on the central Tibetan Plateau (Nam Co Station, 4730 m a.s.l.), Atmos. Res., 153, 155–164, https://doi.org/10.1016/j.atmosres.2014.08.008, 2015.

Wan, X., Kang, S., Li, Q., Rupakheti, D., Zhang, Q., Guo, J., Chen, P., Tripathee, L., Rupakheti, M., Panday, A. K., Wang, W., Kawamura, K., Gao, S., Wu, G., and Cong, Z.: Organic molecular tracers in the atmospheric aerosols from Lumbini, Nepal, in the northern Indo-Gangetic Plain: influence of biomass burning, Atmos. Chem. Phys., 17, 8867–8885, https://doi.org/10.5194/acp-17-8867-2017, 2017.

Wang, G. H., Zhang, R. Y., Gomez, M. E., Yang, L. X., Zamora, M. L., Hu, M., Lin, Y., Peng, J. F., Guo, S., Meng, J. J., Li, J. J., Cheng, C. L., Hu, T. F., Ren, Y. Q., Wang, Y. S., Gao, J., Cao, J. J., An, Z. S., Zhou, W. J., Li, G. H., Wang, J. Y., Tian, P. F., Marrero-Ortiz, W., Secrest, J., Du, Z. F., Zheng, J., Shang, D. J., Zeng, L. M., Shao, M., Wang, W. G., Huang, Y., Wang, Y., Zhu, Y. J., Li, Y. X., Hu, J. X., Pan, B., Cai, L., Cheng, Y. T., Ji, Y. M., Zhang, F., Rosenfeld, D., Liss, P. S., Duce, R. A., Kolb, C. E., and Molina, M. J.: Persistent sulfate formation from London Fog to Chinese haze, P. Natl. Acad. Sci. USA, 113, 13630–13635, https://doi.org/10.1073/pnas.1616540113, 2016.

Wang, J., Ho, S. S. H., Ma, S., Cao, J., Dai, W., Liu, S., Shen, Z., Huang, R., Wang, G., and Han, Y.: Characterization of $PM_{2.5}$ in Guangzhou, China: uses of organic markers for supporting source apportionment, Sci. Total Environ., 550, 961–971, https://doi.org/10.1016/j.scitotenv.2016.01.138, 2016.

Wang, S., Pavuluri, C. M., Ren, L., Fu, P., Zhang, Y.-L., and Liu, C.-Q.: Implications for biomass/coal combustion emissions and secondary formation of carbonaceous aerosols in North China, RSC Adv., 8, 38108–38117, https://doi.org/10.1039/c8ra06127k, 2018.

Wang, Y., Zhuang, G., Tang, A., Yuan, H., Sun, Y., Chen, S., and Zheng, A.: The ion chemistry and the source of $PM_{2.5}$ aerosol in Beijing, Atmos. Environ., 39, 3771–3784, https://doi.org/10.1016/j.atmosenv.2005.03.013, 2005.

Wang, Y., Jia, C., Tao, J., Zhang, L., Liang, X., Ma, J., Gao, H., Huang, T., and Zhang, K.: Chemical characterization and source apportionment of $PM_{2.5}$ in a semi-arid and petrochemical-industrialized city, Northwest China, Sci. Total Environ., 573, 1031–1040, https://doi.org/10.1016/j.scitotenv.2016.08.179, 2016a.

Wang, Y., Jia, C., Tao, J., Zhang, L., Liang, X., Ma, J., Gao, H., Huang, T., and Zhang, K.: Chemical characterization and source apportionment of $PM_{2.5}$ in a semi-arid and petrochemical-industrialized city, Northwest China, Sci. Total Environ., 573, 1031–1040, https://doi.org/10.1016/j.scitotenv.2016.08.179, 2016b.

Wang, Y., Pavuluri, C. M., Fu, P., Li, P., Dong, Z., Xu, Z., Ren, H., Fan, Y., Li, L., Zhang, Y.-L., and Liu, C.-Q.: Characterization of Secondary Organic Aerosol Tracers over Tianjin, North China during Summer to Autumn, ACS Earth Space Chem., 3, 2339–2352, https://doi.org/10.1021/acsearthspacechem.9b00170, 2019.

Wang, Y. J., Dong, Y. P., Feng, J. L., Guan, J. J., Zhao, W., and Li, H. J.: Characteristics and influencing factors of carbonaceous aerosols in $PM_{2.5}$ in Shanghai, China, Huan Jing Ke Xue, 31, 1755–1761, 2010.

Watson, J. G., Chow, J. C., and Houck, J. E.: $PM_{2.5}$ chemical source profiles for vehicle exhaust, vegetative burning, geological material, and coal burning in Northwestern Colorado during 1995, Chemosphere, 43, 1141–1151, https://doi.org/10.1016/S0045-6535(00)00171-5, 2001.

Watson, J. G., Chow, J. C., and Chen, L. W. A.: Summary of Organic and Elemental Carbon/Black Carbon Analysis Methods and Intercomparisons, Aerosol Air Qual. Res., 5, 65–102, https://doi.org/10.4209/aaqr.2005.06.0006, 2005.

Wessels, A., Birmili, W., Albrecht, C., Hellack, B., Jermann, E., Wick, G., Harrison, R. M., and Schins, R. P. F.: Oxidant Generation and Toxicity of Size-Fractionated Ambient Particles in Human Lung Epithelial Cells, Environ. Sci. Technol., 44, 3539–3545, https://doi.org/10.1021/es9036226, 2010.

Widory, D.: Nitrogen isotopes: Tracers of origin and processes affecting PM_{10} in the atmosphere of Paris, Atmos. Environ., 41, 2382–2390, https://doi.org/10.1016/j.atmosenv.2006.11.009, 2007.

Wolfe, A. H. and Patz, J. A.: Reactive Nitrogen and Human Health: Acute and Long-term Implications, Ambio, 31, 120–125, 2002.

Xu, L., Duan, F., He, K., Ma, Y., Zhu, L., Zheng, Y., Huang, T., Kimoto, T., Ma, T., Li, H., Ye, S., Yang, S., Sun, Z., and Xu, B.: Characteristics of the secondary water-soluble ions in a typical autumn haze in Beijing, Environ. Pollut., 227, 296–305, https://doi.org/10.1016/j.envpol.2017.04.076, 2017.

Xu, X. and Zhang, T.: Spatial-temporal variability of $PM_{2.5}$ air quality in Beijing, China during 2013–2018, J. Environ. Manage., 262, 110263, https://doi.org/10.1016/j.jenvman.2020.110263, 2020.

Yan, J., Zhang, M., Jung, J., Lin, Q., Zhao, S., Xu, S., and Chen, L.: Influence on the conversion of DMS to MSA and SO_4^{2-} in the Southern Ocean, Antarctica, Atmos. Environ., 233, 117611, https://doi.org/10.1016/j.atmosenv.2020.117611, 2020.

Yang, F., Huang, L., Duan, F., Zhang, W., He, K., Ma, Y., Brook, J. R., Tan, J., Zhao, Q., and Cheng, Y.: Carbonaceous species in $PM_{2.5}$ at a pair of rural/urban sites in Beijing, 2005–2008, At-

mos. Chem. Phys., 11, 7893–7903, https://doi.org/10.5194/acp-11-7893-2011, 2011.

Yang, H., Yu, J. Z., Ho, S. S. H., Xu, J., Wu, W.-S., Wan, C. H., Wang, X., Wang, X., and Wang, L.: The chemical composition of inorganic and carbonaceous materials in $PM_{2.5}$ in Nanjing, China, Atmos. Environ., 39, 3735–3749, https://doi.org/10.1016/j.atmosenv.2005.03.010, 2005.

Zhang, R., Jing, J., Tao, J., Hsu, S.-C., Wang, G., Cao, J., Lee, C. S. L., Zhu, L., Chen, Z., Zhao, Y., and Shen, Z.: Chemical characterization and source apportionment of $PM_{2.5}$ in Beijing: seasonal perspective, Atmos. Chem. Phys., 13, 7053–7074, https://doi.org/10.5194/acp-13-7053-2013, 2013.

Zhang, Y., Cai, J., Wang, S., He, K., and Zheng, M.: Review of receptor-based source apportionment research of fine particulate matter and its challenges in China, Sci. Total Environ., 586, 917–929, https://doi.org/10.1016/j.scitotenv.2017.02.071, 2017.

Zhao, M., Huang, Z., Qiao, T., Zhang, Y., Xiu, G., and Yu, J.: Chemical characterization, the transport pathways and potential sources of $PM_{2.5}$ in Shanghai: Seasonal variations, Atmos. Res., 158–159, 66–78, https://doi.org/10.1016/j.atmosres.2015.02.003, 2015.

Zhao, P., Dong, F., Yang, Y., He, D., Zhao, X., Zhang, W., Yao, Q., and Liu, H.: Characteristics of carbonaceous aerosol in the region of Beijing, Tianjin, and Hebei, China, Atmos. Environ., 71, 389–398, https://doi.org/10.1016/j.atmosenv.2013.02.010, 2013.